Trabajo de grado

Física
Facultad de Ciencias Naturales y Exactas
Universidad del Valle, sede Cali

Calculation of the domain-length distribution in an isotropic spin-1/2 XX chain

By:
Juan David Álvarez Cuartas

Advisor:
Ph. D. Diego Luis González Cabrera

Santiago de Cali, Junio, 2021

Abstract

We provide a calculation of the first-two spacing distribution for a XX spin-1/2 chain in the presence of an external magnetic field based on its Toeplitz determinant representation and the fermion formalism. The equivalence between the analytical expressions for the spacing-distributions provided by the second quantization formalism and those from the inter-particle distribution method is illustrated. The results obtained for the spacing-distributions are used to describe the magnetic behavior of the system and contrasted with the standard analysis based on quantities such as the average energy, magnetization and susceptibility. We provide an extensive explanation of the application of the Stochastic Series Expansion method to the XX model for the code implementation of the Quantum Monte Carlo method. Finally, the results obtained from analytical expressions are compared with those from extensive Quantum Monte Carlo simulations.

Keywords: Spacing distribution, spin-1/2 chain, Toeplitz determinant, fermion formalism, IPDF method, Stochastic Series Expansion Quantum Monte Carlo, zero temperature, finite temperature.

Resumen

Proporcionamos un cálculo de la dos primeras distribuciones de espaciamiento para una cadena de espines 1/2 XX en presencia de un campo magnético externo basado en su representación como determinante de Toeplitz y el formalismo de fermiones. Se ilustra la equivalencia entre las expresiones analíticas para las distribuciones de espaciamiento proporcionadas por el formalismo de segunda cuantización y las del método de distribución interpartícula. Los resultados obtenidos para las distribuciones de espaciamiento se utilizan para describir el comportamiento del sistema debido al campo magnético y se contrastan con el análisis estándar basado en cantidades termodinámicas como la energía promedio, magnetización y susceptibilidad. Proporcionamos una explicación extensa de la aplicación del método de expansión de series estocásticas al modelo XX para la implementación en código del método Monte Carlo cuántico. Finalmente, los resultados obtenidos de expresiones analíticas se comparan con los de extensas simulaciones de Monte Carlo cuántico.

Palabras clave: Distribución de espaciamiento, cadena de espín 1/2, determinante de Toeplitz, formalismo de fermiones, método de IPDF, Método de Monte Carlo cuántico basado en expansión de series estocásticas, temperatura cero, temperatura finita.

List of Figures

List of Tables

List of Symbols

Below are included general symbols, as Greek and Latin letters, subscripts, and abbreviations that will be used in the present document.

Symbols with Latin letters

Symbol	Term	Definition
$\mathbb{C}^2$	Spin-1/2 space state	
$\mathscr{E}$	Space of states	
$\hat{x}, \hat{y}, \hat{z}$	Lattice axis	
J	Coupling constant	
J_α	Coupling constant for α axis	
$\hat{S}_j^\alpha$	Spin operator on site j for α axis	
$\hat{S}_j^\pm$	Ladder operators on site j	$\hat{S}_j^\pm = \hat{S}_j^x \pm i\hat{S}_j^y$
$\vec{h}$	Magnetic field	$\vec{h} = h\hat{z}$
h	Magnitude of magnetic field	
h_c	Magnitude of critical magnetic field	$h_c = J/2$
$\hat{\mathcal{H}}$	Hamiltonian operator	
$\hat{I}$	Identity operator	
i	Imaginary unit	$i = \sqrt{-1}$
$\hat{c}_j, \hat{c}_j^\dagger$	Fermion operators	
$\hat{C}_j, \hat{C}_j^\dagger$	Fourier transform of the fermion operators	
$\hat{n}_q$	Fermion occupation number operator	$\hat{n}_q = \hat{C}_q^\dagger \hat{C}_q$
N	Chain size	
M	Number of spins pointing down	
$\mathcal{Z}_N(\beta)$	Partition function	
k_f	Fermi radius	$k_f = \cos^{-1}(2h/J)$
T	Temperature	
k_B	Boltzmann constant	

$\langle E \rangle$	Average energy per particle	$-\partial_\beta \ln \mathcal{Z}_N(\beta)$
$\mathcal{F}$	Free energy per particle	$\mathcal{F} = -k_B T \ln \mathcal{Z}_N(\beta)$
$\mathcal{C}$	Heat capacity per particle	$\partial_T \langle E \rangle$
$\mathcal{M}$	Magnetization per particle	$\mathcal{M} = -\partial_h \mathcal{F}$
$\mathcal{X}$	Magnetic susceptibility per particle	$\mathcal{X} = \partial_h \mathcal{M}$
$\hat{P}_j$	Spin-up projector operator	$\hat{P}_j = \hat{S}_j^z + \frac{\hat{I}}{2}$
$P(n)$	Emptiness formation probability	$P(n) = \left\langle \prod_{j=1}^{n} \hat{P}_j \right\rangle$
n	Domain size	
p_n^m	m-th spacing-distribution	
$\mathcal{P}$	Represents a probability	
p_n^0	First spacing-distribution	$p_n^0 = \mathcal{P}(\bullet \overbrace{\circ \cdots \circ}^{m} \bullet)$
$Q(L)$	Two consecutive domain length distribution	$Q(L) = \sum_{l=1}^{L} \mathcal{P}(\bullet \overbrace{\circ \cdots \circ}^{l} \overbrace{\bullet \cdots \bullet}^{L-l} \circ)$
p_n^1	Second spacing-distribution	$p_n^1 = \sum_m \mathcal{P}(\bullet \overbrace{\circ \cdots \circ}^{m-1} \bullet \overbrace{\circ \cdots \circ \cdots \circ}^{n-m-1} \bullet)$
$\mathcal{O}$	Product of hole operators	$\mathcal{O} = \prod_{l=1}^{n-1} \hat{b}_l^\dagger \hat{b}_l$
$\hat{\mathcal{Q}}$	Product of particle operators	$\hat{\mathcal{Q}}_{l+1}^{L} = \prod_{j=l+1}^{L} \hat{c}_j^\dagger \hat{c}_j$
$\hat{A}$	Any arbitrary observable	
$\mathcal{W}\{\alpha\}$	Weight of the configuration α	
$A(x \to x')$	Probability of acceptance of the update x to x'	
b	bond	
h_b	Magnetic field	$h_b = h/2b$
nh	Cutoff of the expansion	
f	Any arbitrary function	

Symbols with Greek letters

Symbol	Term	Definition
Δ	Coupling constant for $\hat{z}$ axis	$\Delta = J_z/J$
δ_{kl}	Kronecker delta	
$\epsilon_{\alpha\beta\gamma}$	Levi-Civita symbol	
π		
$\epsilon(q)$	Energy in the thermodynamic limit	$\epsilon(q) = 2h - J\cos q$
ϵ_l	Energy for even states	$\epsilon_l = 2h - J\cos(2\pi l/N)$
Δq	Lattice site in the reciprocal space	$\Delta q = 2\pi/N$

Símbolo	Término	Definición
β	Inverse temperature	$\beta = 1/T$
α	Arbitrary configuration of the configuration space	
ϵ	Excess over the minimum value	
τ	Computational cost	

Abbreviations

Abbreviation	Term
QIS	Quantum Inverse Scattering method
JWT	Jordan-Wigner transformation
GS	Ground State
PBC	Periodic Boundary Conditions
ABC	Antiperiodic Boundary Conditions
EFP	Emptiness Formation Probability
IPDF	Interparticle Distribution Function
WS	Wigner surmise
GWS	Generalized Wigner surmise
SSE	Stochastic Series Expansion
QMC	Quantum Monte Carlo
MCS	Monte Carlo sweeps

Introduction

Many-body interacting systems, except for a few specific cases, are usually complicated to study both classically and quantum. The ones with an exact solution generally involve complex analytic expressions that make it hard to calculate the physical quantities of interest [4–7]. Systems of this type that have an analytic solution are called *integrable systems*. Unfortunately, the majority of interacting many-body systems do not have known exact solutions.

In a few words, the spin chain are systems with rich theoretical properties that in themselves are reason enough to be widely studied since 1928 when Heisenberg proposes a model for explaining the ferromagnetism [8]. However, in the present, this kind of model keep being widely studied for their applications, a few of many examples are in quantum computing [9, 10], for example, the implementation of communication protocols [11, 12] and the transfer of states between this systems [13, 14], in addition to novel implementations in ultracold atom systems and the manufacturing on nanodevices [15, 16].

The one-dimensional isotropic XX model is an integrable system and is a good starting point to study many-body interacting systems [4, 17]. One quantity of interest that is easy to calculate for this system is a correlation function called *Emptiness Formation Probability* (EFP), $P(n)$ [18]. By definition, $P(n)$ is the probability of having n consecutive sites of the lattice with spins up. In the context of the more general XXZ model, there are many works that have studied the main properties of this correlation function using analytic tools [5, 19, 20]. It has been possible to obtain analytic solutions in terms of Fredholm determinants, multiple-integrals representations [20, 21], and the representation as Toeplitz determinant. The last tool is of special interest for the case of the XX model and is used in this work to study of the asymptotic behavior of $P(n)$ for arbitrary values of temperature [17].

On the other hand, the method called "*Interparticle Distribution Function*" (IPDF) is a technique well known and widely used in the study of reaction-diffusion systems [22]. For example, the IPDF method can be used to describe coalescence processes in one-dimensional systems [23–25]. The fundamental idea of the IPDF method is to describe the structure of the one-dimensional systems through correlations written in terms of $P(n)$. In this work we calculate the first two spacing distributions between the consecutive domain borders $p^{(0)}(n)$ and $p^{(1)}(n)$ for an isotropic spin-1/2 chain XX. As usual, $p^{(0)}(n)$ is the probability that the distance between the borders of one domain be n while $p^{(1)}(n)$ is the probability that the distance between the borders of two consecutive domains be n [26].

Finally, we perform a computational simulation based on the *Quantum Monte Carlo* (QMC) method to validate the theoretical results. QMC is a family of numerical methods widely used to study complex quantum systems, usually, unsolvable analytically. It allows us to obtain precise solutions for many-body problems. In particular, with the traditional QMC we can study the ground state of the d-dimensional many-particle system by an equivalent Ising like in $(d+1)$-dimension at finite temperature [27]. One of the most used variants of the Quantum Monte Carlo method is based on the expansion of the Boltzmann

factor and is known as "*Stochastic Series Expansion*" (SSE) [1]. The SSE method can be applied to a wide variety of systems and is quite efficient thanks to the traces are sampled using non-local updates [2, 28].

This thesis is divided as follows. In the chapter 1, we write the Hamiltonian of the XX model. To diagonalize the Hamiltonian we use the Jordan-Wigner transformation (JWT) mapping the spin system onto an equivalent free fermion system . Then, we calculate the partition function and some thermodynamic quantities as illustration. In the chapter 2, once we have exposed the main properties of the system, we will focus our attention on the calculation and analysis of the emptiness distribution $P(n)$. Some known results based on the Toeplitz determinant representation of $P(n)$ are discussed. In chapter 3, we introduce the basic concepts of the IPDF method, and calculate the first two spacing distributions, P_n^0 and P_n^1. In chapter 4, we present of the SSE QMC method, providing a derivation of the expressions used in the simulation and the details of the code implementation. In chapter 5, we present the results obtained from the computational simulation. Finally, in chapter 6 we provide a summary of the thesis.

Contents

Chapter 1

The XX model

In this chapter, we present a simple and general model for a one-dimensional isotropic spin-$1/2$ chain. All the terms that compose the Hamiltonian of the system are explained. Then, we consider a particular case the XX model. The ladder operators are introduced to write the Hamiltonian in a more convenient form, later we introduce the Jordan-Wigner transformation (JWT) to map the spin system onto free fermion system. The equivalent Hamiltonian associated to free fermions is diagonalized by using the Fourier transform (FT) of the fermionic operators. Then, we calculate the partition function in the canonical ensemble with periodic boundary conditions (PBC). Finally, we calculate the ground state of the system and some thermodynamic quantities using the partition function.

1.1 Derivation of the XX chain Hamiltonian

Quantum integrability in (1+1)-dimension has been fascinating topic research, especially after the seminal works on the quantization of the Lie groups and its application to lattice systems performed by the St. Petersburg group [29–32], the development of the "*Quantum Inverse Scattering*" (QIS) method [5], and other techniques as the Bethe ansatz [33, 34], among others. Also there are many works focused on the study of integrable models [35] and applications to condensed matter physics [36, 37].

A spin chain is a lattice of objects, can be atoms, which have a degree of freedom called spin. The nature of the spin-spin interaction is determined merely by quantum phenomena. Due to the dominant coupling between two dipoles, there is an interaction between adjacent spins [38].

The proposed model is composed by a one-dimensional lattice with periodic boundary conditions. At each lattice site there is an object with spin-$1/2$ which is free to rotate. Mathematically, this system is represented by a local space of states $\mathbb{C}^2$ in which the spins possess two possible configurations: "spin-up" and "spin-down". The corresponding matrix representation of these states is given by

$$|\uparrow\rangle \equiv |+\rangle = \begin{pmatrix} 1 \\ 0 \end{pmatrix} \quad \text{and} \quad |\downarrow\rangle \equiv |-\rangle = \begin{pmatrix} 0 \\ 1 \end{pmatrix}. \tag{1-1}$$

The complete state space, $\mathscr{E}$, consist of the tensorial product of the spin-up and spin-down states over all the sites of the lattice

$$\mathscr{E} = \mathbb{C}^2 \otimes \mathbb{C}^2 \otimes \cdots \otimes \mathbb{C}^2. \tag{1-2}$$

The XYZ Hamiltonian corresponding to a system of N spins with nearest-neighbor interactions in the $\hat{x}$, $\hat{y}$ and $\hat{z}$ axis, is given by

$$\hat{\mathcal{H}}_{XYZ} = \sum_{j=1}^{N} \left(J_x \hat{S}_j^x \hat{S}_{j+1}^x + J_y \hat{S}_j^y \hat{S}_{j+1}^y + J_z \hat{S}_j^z \hat{S}_{j+1}^z \right) - 2h \sum_{j=1}^{N} \hat{S}_j^z, \tag{1-3}$$

where the constant J_α represents the coupling associated to the spin-spin interaction in the α axis, with $\alpha = \hat{x}, \hat{y}$ or $\hat{z}$. As usual, $\hat{S}_j^\alpha$ is a spin operator acting on the site j of the α axis. The last term represents the system interaction with an external magnetic field $\vec{h} = h\hat{z}$.

The called XXZ model differs from the previous one for the introduction of a parameter, Δ, that measures the anisotropy of the system Δ along the $\hat{z}$ axis. For this model, the Hamiltonian can be written as

$$\hat{\mathcal{H}}_{XXZ} = J \sum_{j=1}^{N} \left(\hat{S}_j^x \hat{S}_{j+1}^x + \hat{S}_j^y \hat{S}_{j+1}^y + \Delta \hat{S}_j^z \hat{S}_{j+1}^z \right) - 2h \sum_{j=1}^{N} \hat{S}_j^z. \tag{1-4}$$

In the XXZ model $J_x = J_y = J$ and $J_z = J\Delta$. The Hamiltonian of the XX model is a particular case of the XXZ model, where $\Delta = 0$.

$$\hat{\mathcal{H}}_{XX} = J \sum_{j=1}^{N} \left(\hat{S}_j^x \hat{S}_{j+1}^x + \hat{S}_j^y \hat{S}_{j+1}^y \right) - 2h \sum_{j=1}^{N} \hat{S}_j^z. \tag{1-5}$$

As was mentioned before, periodic boundary conditions are assumed, that is $S_{N+1}^\alpha \equiv S_1^\alpha$. For the particular case of spin-$1/2$ the operators S_j^α can be represented by the Pauli matrices. Therefore, these operators satisfy the following commutation relations

$$\left[\hat{S}_k^\alpha, \hat{S}_l^\beta \right] = i\, \delta_{kl}\, \epsilon_{\alpha\beta\gamma}\, \hat{S}_k^\gamma. \tag{1-6}$$

Observe that for $h = 0$ the Hamiltonian preserves the total magnetization along the $\hat{z}$ axis, that is $[\hat{\mathcal{H}}, \hat{S}^z] = 0$.

1.2 Diagonalization of the XX Hamiltonian

Diagonal operators are useful since they give us not only information of which state the system could be after a measurement is performed, but also the corresponding energy of that state. In this way, a diagonalized Hamiltonian make easier the calculation of the physical quantities of the system. In order to accomplish that for our XX chain, the Hamiltonian (1-5) will be rewritten in terms of the ladder operators. Then, the JWT (see Appendix A) is used to map the spin system onto a free-fermion one which can be diagonalized using Fourier transform [4].

1.2.1 XX Hamiltonian in terms of ladder operators

Consider the Hamiltonian given by Eq. (1-5) with periodic boundary conditions

$$\hat{\mathcal{H}}_{XX} = J\sum_{i=1}^{N}\left(\hat{S}_j^x\hat{S}_{j+1}^x + \hat{S}_j^y\hat{S}_{j+1}^y\right) - 2h\sum_{j=1}^{N}\hat{S}_j^z, \quad \hat{S}_{N+1}^{\alpha} \equiv \hat{S}_1^{\alpha}, \tag{1-7}$$

whose operators satisfies the anti-commutation relation given by Eq. (1-6). Since each site of the lattice has two possible states, “spin-up” or “spin-down”, for this Hamiltonian there are a total of 2^N states. The ladder operators for the spin operators are defined according to

$$\hat{S}_k^{\pm} \equiv \hat{S}_k^x \pm i\hat{S}_k^y. \tag{1-8}$$

The $SU(2)$ algebra is defined by the generators $\hat{S}^{\pm}$, $\hat{S}^z$ and the exchange relations [39]

$$[\hat{S}^+, \hat{S}^-] = 2\hat{S}^z, \quad \text{and} \quad [\hat{S}^z, \hat{S}^{\pm}] = \pm\hat{S}^{\pm}. \tag{1-9}$$

The spin-$1/2$ representation of $SU(2)$ maps the three generators of the algebra to the three Pauli matrices [39, 40]. Then, the Pauli matrices and the spin operators are related as follows

$$\hat{S}^x = \frac{1}{2}\begin{pmatrix}0 & 1\\ 1 & 0\end{pmatrix}, \quad \hat{S}^y = \frac{1}{2}\begin{pmatrix}0 & -i\\ i & 0\end{pmatrix}, \quad \text{and} \quad \hat{S}^z = \frac{1}{2}\begin{pmatrix}1 & 0\\ 0 & -1\end{pmatrix}. \tag{1-10}$$

The action of the operator $\hat{S}_j^+$ ladder operators over a eigenstate of $\hat{S}_j^z$ is simply

$$\hat{S}_j^+\left|\cdots\uparrow\cdots\right\rangle = 0 \quad \text{and} \quad \hat{S}_j^+\left|\cdots\downarrow\cdots\right\rangle = \left|\cdots\uparrow\cdots\right\rangle, \tag{1-11}$$

while the operator $\hat{S}_j^-$ acts as follows

$$\hat{S}_j^-\left|\cdots\uparrow\cdots\right\rangle = \left|\cdots\downarrow\cdots\right\rangle \quad \text{and} \quad \hat{S}_j^-\left|\cdots\downarrow\cdots\right\rangle = 0. \tag{1-12}$$

Moreover, the consecutive action of the two operators $\hat{S}_j^+\hat{S}_j^-$ over a eigenstate of $\hat{S}_j^z$ is simply

$$\hat{S}_j^+\hat{S}_j^-\left|\cdots\uparrow\cdots\right\rangle = \left|\cdots\uparrow\cdots\right\rangle \quad \text{and} \quad \hat{S}_j^+\hat{S}_j^-\left|\cdots\downarrow\cdots\right\rangle = 0, \tag{1-13}$$

Therefore, the expected value of the number operator $\hat{\mathcal{N}} = \sum_{j=1}^{N}\hat{S}_j^+\hat{S}_j^-$ gives the total number of spins pointing up, M. In terms of the ladder operators the Hamiltonian given by Eq. (1-7) can be written as

$$\begin{aligned}\hat{\mathcal{H}}_{XX} &= J\sum_{j=1}^{N}\left[\left(\frac{\hat{S}_j^+ + \hat{S}_j^-}{2}\right)\left(\frac{\hat{S}_{j+1}^+ + \hat{S}_{j+1}^-}{2}\right) + \left(\frac{\hat{S}_j^+ - \hat{S}_j^-}{2i}\right)\left(\frac{\hat{S}_{j+1}^+ + \hat{S}_{j+1}^-}{2i}\right)\right] - 2h\sum_{j=1}^{N}\hat{S}_j^z \\ &= J\sum_{j=1}^{N}\left[\frac{1}{4}\left(\hat{S}_j^+\hat{S}_{j+1}^+ + \hat{S}_j^+\hat{S}_{j+1}^- + \hat{S}_j^-\hat{S}_{j+1}^+ + \hat{S}_j^-\hat{S}_{j+1}^-\right)\right. \\ &\qquad \left. -\frac{1}{4}\left(\hat{S}_j^+\hat{S}_{j+1}^+ - \hat{S}_j^+\hat{S}_{j+1}^- - \hat{S}_j^-\hat{S}_{j+1}^+ + \hat{S}_j^-\hat{S}_{j+1}^-\right)\right] - 2h\sum_{j=1}^{N}\hat{S}_j^z \\ &= \frac{J}{2}\sum_{j=1}^{N}\left(\hat{S}_j^+\hat{S}_{j+1}^- + \hat{S}_j^-\hat{S}_{j+1}^+\right) - 2h\sum_{j=1}^{N}\hat{S}_j^z. \end{aligned} \tag{1-14}$$

It is easy to see that the ladder operators satisfy the following algebra

$$\{\hat{S}_j^+, \hat{S}_j^-\} = \hat{I} \quad \text{and} \quad [\hat{S}_i^+, \hat{S}_j^-] = 0. \tag{1-15}$$

Note that it is quite inconvenient to work directly with ladder operators because the first relation in Eq. (1-15) is a fermionic relation while the second is bosonic.

1.2.2 Mapping the spin-1/2 system onto free fermions

The Hamiltonian given by Eq. (1-14) can be written as the sum of three Hamiltonians that represents different interactions as follows

$$\hat{\mathcal{H}}_{XX} = \hat{\mathcal{H}}_0 + \hat{\mathcal{H}}_b + \hat{\mathcal{H}}_z, \tag{1-16}$$

where, the first term of Eq. (1-14) have been divided into two terms, the first one, $\hat{\mathcal{H}}_0$ which describes the nearest-neighbor interaction except in the boundary, and the second one $\hat{\mathcal{H}}_b$ which describes the contribution of the boundary conditions, i.e., the interaction between spins in site N and 1. Finally, $\hat{\mathcal{H}}_z$, describes the interaction with the external magnetic field h. Then, using the Jordan-Wigner transformation (JWT) given by Eqs. (A-11) and (A-12), the terms of Eq. (1-16) transform as follows

$$\begin{aligned}\hat{\mathcal{H}}_0 &= \frac{J}{2}\sum_{j=1}^{N-1}\left(\hat{S}_j^+\hat{S}_{j+1}^- + \hat{S}_j^-\hat{S}_{j+1}^+\right) \\ &= -\frac{J}{2}\sum_{j=1}^{N-1}\left(\hat{c}_{j+1}^\dagger\hat{c}_j + \hat{c}_j^\dagger\hat{c}_{j+1}\right). \end{aligned} \tag{1-17}$$

Similarly, using the JWT and taking into account the boundary conditions given by $\hat{S}_{N+1}^\alpha \equiv \hat{S}_1^\alpha$ we obtain that $\hat{\mathcal{H}}_b$ can be written as

$$\begin{aligned}\hat{\mathcal{H}}_b &= \frac{J}{2}\left(\hat{S}_N^+\hat{S}_1^- + \hat{S}_N^-\hat{S}_1^+\right) \\ &= \frac{J}{2}\left(\hat{c}_N^\dagger\hat{c}_1 + \hat{c}_N\hat{c}_1^\dagger\right)e^{i\pi M} \\ &= \frac{J}{2}(-1)^M\left(\hat{c}_N^\dagger\hat{c}_1 + \hat{c}_N\hat{c}_1^\dagger\right)\end{aligned} \tag{1-18}$$

We remark that the sign of the Hamiltonian given by Eq. (1-18) depends on the parity of the number of spins down M. In fact, in the fermion representation the boundary conditions implies $\hat{c}_{N+1}^\dagger = \pm\hat{c}_1^\dagger$, where the upper and lower signs correspond to M even (antiperiodic boundary conditions ABC) and odd (periodic boundary conditions PBC), respectively. Finally, the $\hat{H}_z$ term is given by

$$\begin{aligned}\hat{\mathcal{H}}_z &= -2h\sum_{j=1}^{N}\hat{S}_j^z \\ &= -2h\sum_{j=1}^{N}\left(\frac{\hat{I}}{2} - \hat{c}_j^\dagger\hat{c}_j\right).\end{aligned} \tag{1-19}$$

It is not difficult to see that Eq. (1-19) has the same matricial representation of $\hat{S}^z$ given in Eq. (1-10). Replacing Eqs. (1-17), (1-18) and (1-19) in Eq. (1-14) we obtain

$$\hat{\mathcal{H}}_{XX} = -\frac{J}{2}\sum_{j=1}^{N-1}(\hat{c}_j^\dagger\hat{c}_{j+1} + \hat{c}_j\hat{c}_{j+1}^\dagger) + \frac{J}{2}(-1)^M\left(\hat{c}_N^\dagger\hat{c}_1 + \hat{c}_N\hat{c}_1^\dagger\right) - hN + 2h\sum_{j=1}^{N}\hat{c}_j^\dagger\hat{c}_j. \tag{1-20}$$

The first two terms of Eq. (1-20) describe the spin-spin interaction, the next one is the contribution due to the boundary conditions and the last two terms are associated to the interaction with the external magnetic field.

The JWT is used to 'fix' the canonical commutation relations so that the spin-statistic theorem holds as it was shown in the previous subsection. The JWT has very strong physical consequences because implies there is not distinction between spin-1/2 particles and fermions. As shown in this section, we can represent a spin system such as the one described by Eq. (1-7) by means of an equivalent fermion system as the one given by Eq. (1-20).

1.2.3 Diagonalization using the Fourier transform

Lets introduce the Fourier transform for the fermionic operators as follows

$$\hat{C}_q = \frac{1}{\sqrt{N}}\sum_{j=1}^{N}e^{-iqj}\hat{c}_j, \quad \text{and} \quad \hat{C}_q^\dagger = \frac{1}{\sqrt{N}}\sum_{j=1}^{N}e^{iqj}\hat{c}_j, \tag{1-21}$$

where we define the discretization of the lattice in the reciprocal space as $q = 2\pi n/N$, where n is integer for PBC (M odd) and n is half-integer for ABC (M even). Applying the transformations given by Eq. (1-21) to the Hamiltonian given by Eq. (1-20) we obtain

$$\begin{aligned}\hat{\mathcal{H}}_{XX} &= -\frac{J}{2}\sum_q \left((e^{iq}+e^{-iq})\hat{C}_q^\dagger \hat{C}_{q+1}\right) - hN + 2h\sum_q \hat{C}_q^\dagger \hat{C}_q \\ &= \sum_q (2h - J\cos q)\hat{C}_q^\dagger \hat{C}_q - hN \\ &= \sum_q \epsilon(q)\hat{n}_q - hN, \end{aligned} \tag{1-22}$$

where we have defined $\epsilon(q) = 2h - J\cos q$, which physically corresponds to the energy of the system, and $\hat{n}_q = \hat{C}_q^\dagger \hat{C}_q$ is the fermionic occupation number. We remark that the first term contributes to the Hamiltonian depending on the value of the occupation number for each site q, instead, the second term depends on the total number of sites N and the magnitude of the magnetic field h.

As mentioned before for $h = 0$ the magnetization is conserved. In the fermionic picture, this symmetry is manifested as conservation of the total fermion number, that is $[\hat{\mathcal{H}}_{XX}, \sum_i \hat{n}_i] = 0$.

1.3 Partition function

The statistical information of a thermodynamic system in equilibrium is contained in the partition function $\mathcal{Z}_N(\beta)$. Therefore, from $\mathcal{Z}_N(\beta)$ it is possible to calculate several thermodynamic observables such as the internal energy, heat capacity, magnetization, susceptibility, etc. The partition function can be calculated by the sum of the Boltzmann factor over all accessible microstates. Let $\mathcal{Z}_\mu(\beta)$ be the partition function for a given number of fermions (magnetization). The number of states with a given magnetization is $N/M!/(N-M)!$. Remembering that the number of fermions goes from 0 to N, the partition function of the system can be written as

$$\begin{aligned}\mathcal{Z}_N(\beta) &= \sum_{\mu=0}^{N} \mathcal{Z}_\mu(\beta) \\ &= \sum_{\mu=0}^{N} {\sum_{\{n_q\}}}' e^{-\beta\sum_q (2h - J\cos q))n_q + \beta\, h\, N}. \end{aligned} \tag{1-23}$$

In order to simply the notation we define $z = e^{-2\beta h}$. The sum over the occupation numbers satisfies the conditions $n_q = 0, 1$ and $\sum_q n_q = \mu$. The second condition can be written explicitly by using a Kronecker delta

$$\mathcal{Z}_N(\beta) = \sum_{\mu=0}^{N} {\sum_{\{n_q\}}}'' z^{-\frac{N}{2}} e^{-\beta\sum_q (2h - J\cos(q))n_q} \delta_{\sum_p n_p, \mu}, \tag{1-24}$$

In this way the sum over n_q, $\sum_{\{n_q\}}$, just include the condition $n_q = 0, 1$. The boundary conditions depend on the parity of the number of fermions (spins down), M. This fact is reflected on the partition function too because there are two sets of q: q_{even} and q_{odd}. Therefore, in the calculation of the sums in Eq. (1-24) we have to consider carefully both cases

$$\mathcal{Z}_N(\beta) = \sum_{\mu=0}^{N} {\sum_{\{n_q\}}}'' \left[z^{-\frac{N}{2}} \xi_1 \prod_{q_{even}} e^{\beta J \cos(q) n_q} + z^{-\frac{N}{2}} \xi_2 \prod_{q_{odd}} e^{\beta J \cos(q) n_q} \right] \delta_{\sum_p n_p, \mu}, \tag{1-25}$$

with

$$\xi_1 = \frac{z^M + (-z)^M}{2} \quad \text{and} \quad \xi_2 = \frac{z^M - (-z)^M}{2}, \tag{1-26}$$

The partition function has been written in such way that for M even only the first term remains ($\xi_1 = 1$ and $\xi_2 = 0$). Analogously, for M odd just the second term remains ($\xi_1 = 0$ and $\xi_2 = 1$). Performing the sum over μ we obtain

$$\begin{aligned} \mathcal{Z}_N(\beta) \;=\; & \frac{z^{-\frac{N}{2}}}{2} \left[\sum_{\{n_q\}} \prod_{q_{even}} e^{\beta(J\cos q - 2h) n_q} + \sum_{\{n_q\}} \prod_{q_{even}} e^{\beta(J\cos q - 2h) n_q} (-1)^{n_q} \right. \\ & \left. + \sum_{\{n_q\}} \prod_{q_{odd}} e^{\beta(J\cos q - 2h) n_q} - \sum_{\{n_q\}} \prod_{q_{odd}} e^{\beta(J\cos q - 2h) n_q} (-1)^{n_q} \right]. \end{aligned} \tag{1-27}$$

Given that we are working with fermions we have that the occupation number for a given site only have two possible values, $n_q = \{0, 1\}$, thus, the Eq. (1-27) transforms as follows

$$\begin{aligned} \mathcal{Z}_N(\beta) \;=\; & \frac{z^{-N/2}}{2} \left(\prod_{l=1}^{N} \left(1 + z e^{f(q_{odd})}\right) - \prod_{l=1}^{N} \left(1 - z e^{f(q_{odd})}\right) \right. \\ & \left. + \prod_{l=1}^{N} \left(1 + z e^{f(q_{even})}\right) + \prod_{l=1}^{N} \left(1 - z e^{f(q_{even})}\right) \right), \end{aligned} \tag{1-28}$$

where $q_{even} = 2\pi l/N$ and $q_{odd} = \pi(2l-1)/N$ and $f(q) = \beta J \cos(q)$. Finally, the partition function consists of four terms, the first two corresponds to the even states and the last two to the odd states, in each pair of term the second one corresponds to the contribution of the boundary conditions to the partition function. Therefore, in the thermodynamic limit these terms vanish.

1.4 Thermodynamic observables

Now we proceed to calculate some thermodynamic quantities. First at all, in order to simplify the calculation we remark that the observables will be calculated in the thermodynamic limit from the partition function $\mathcal{Z}_N(\beta)$. In this limit $N \to \infty$, then

$$\lim_{N\to\infty} e^{-\beta J \cos(2\pi l/N)} = \lim_{N\to\infty} e^{-\beta J \cos(\pi(2l-1)/N)} = e^{-\beta J \cos(2\pi l/N)}.$$

Therefore, the product in the second and fourth terms of Eq. (1-28) vanish. Note that these terms are associated to the boundary conditions and, therefore, they do not contribute in the thermodynamic limit. Consequently, in the thermodynamic limit due to the great number of sites there is not distinction between even and odd states, they contribute equally to the partition function. Therefore, the partition function takes the form

$$\mathcal{Z}_N(\beta) = z^{-\frac{N}{2}} \prod_{l=1}^{N} \left(1 + z^{-N/2} e^{-\beta J \cos q_l}\right). \tag{1-29}$$

1.4.1 Internal energy

The internal energy per site can be calculated from the partition function as follows

$$\begin{aligned} \langle E \rangle &= -\frac{1}{N} \frac{\partial \ln \mathcal{Z}_N(\beta)}{\partial \beta} \\ &= -\frac{1}{N} \frac{\partial}{\partial \beta} \ln \left(z^{-N/2} \left[\prod_{l=1}^{N} \left(1 + z\, e^{J\beta \cos q_l}\right) \right] \right). \end{aligned}$$

The derivatives of the two factors in Eq. (1-30) can be calculated

$$\frac{\partial}{\partial \beta} \frac{\ln z^{-N/2}}{2} = \frac{\partial}{\partial \beta} e^{hN/T} = \frac{\partial}{\partial \beta}(hN\beta) = hN, \tag{1-30}$$

and

$$\begin{aligned} \frac{\partial}{\partial \beta} \ln \left[\prod_{l=1}^{N} \left(1 + e^{\epsilon(q_l)\beta}\right) \right] &= \frac{\partial}{\partial \beta} \ln \left[\prod_{l=1}^{N} \left(1 + e^{\epsilon(q_l)\beta}\right) \right] \\ &= \sum_{l=1}^{N} \frac{\partial}{\partial \beta} \ln \left(1 + e^{\epsilon(q_l)\beta}\right) \\ &= \sum_{l=1}^{N} \frac{\epsilon(q_l) e^{-\beta \epsilon_l}}{1 + e^{-\beta \epsilon(q_l)}}, \end{aligned} \tag{1-31}$$

where we have define $\epsilon(q_l) = 2h - J\cos(2\pi l/N)$. Finally, replacing Eq. (1-30) and Eq. (1-31) in Eq. (1-30) the internal energy takes the form

$$\langle E \rangle = -h - \frac{1}{N} \sum_{l=1}^{N} \frac{\epsilon(q_l) e^{-\beta \epsilon(q_l)}}{1 + e^{-\beta \epsilon(q_l)}}.$$

In the thermodynamic limit the discrete sum converges to an integral

$$\frac{1}{\Delta q}\sum_{l=1}^{N}\Delta q = \frac{N}{2\pi}\int_{-k_f}^{k_f} dq, \quad \text{with} \quad \Delta q = \frac{2\pi}{N}, \tag{1-32}$$

where the limits of the integral are given by the Fermi's radius k_f, that separates the occupied from the non-occupied states, at zero-temperature. The Fermi radius is related to the system parameters as well, to find the relation we need to take into account that in the Fermi edges the energy $\epsilon(q)$ must be zero

$$k_f = \cos^{-1}\left(\frac{2h}{J}\right). \tag{1-33}$$

It is easy to see that $k_f \to 0$ as $h \to J/2 \equiv h_c$, such h_c and is called critical magnetic field. Therefore, in the thermodynamic limit Eq. (1-32) can be written as

$$\langle E\rangle = \left\langle \hat{H}\right\rangle = -h + \int_{-\pi}^{\pi}\frac{dq}{2\pi}\frac{\epsilon(q)e^{-\beta\epsilon(q)}}{1+e^{-\beta\epsilon(q)}}. \tag{1-34}$$

The energy per particle of the ground state of the system, i.e., the state of the system at zero temperature is given by

$$E_g = \langle GS|\,\hat{\mathcal{H}}\,|GS\rangle = -h\left(1-\frac{2M}{N}\right) + \frac{J}{\pi}\sin\left(\frac{\pi M}{N}\right), \tag{1-35}$$

where $|GS\rangle$ represents the ground state, obtained from a iterative application of the creation operator $\hat{C}_q^\dagger$ to the vacuum state $|0\rangle$ as follows

$$|GS\rangle = \prod_q \hat{C}_q^\dagger\,|0\rangle\,. \tag{1-36}$$

From Eq. (1-35) it is clear that at $T=0$, for $h \geq J/2$ we have $M/N \to 0$ $E_g = -h$. In contrast, for $h \to 0$, $M/N \to 1/2$ and $E_g \to J/\pi$.

1.4.2 Free energy, heat capacity, magnetization and magnetic susceptibility

The free energy per lattice site can be easily calculated from partition function as follows

$$\begin{aligned}\mathcal{F} &= -\frac{k_BT}{N}\ln\mathcal{Z}_N(\beta)\\ &= -\frac{T}{N}\left(\frac{hN}{T}+\sum_{l=1}^{N}\ln(1+e^{-\beta\epsilon(q)})\right)\\ &= -h - k_BT\int_{-\pi}^{\pi}\frac{dq}{2\pi}\ln(1+e^{-\beta\epsilon(q)}).\end{aligned}$$

where in the last line we have taken the thermodynamic limit. The heat capacity per lattice site can be calculated using the average energy as follows

$$\begin{aligned}
\mathcal{C} &= \frac{\partial}{\partial T}\langle E\rangle \\
&= \frac{\partial}{\partial T}\left(-h+\int_{-\pi}^{\pi}\frac{dq}{2\pi}\frac{\epsilon(q)e^{-\beta\epsilon(q)}}{1+e^{-\beta\epsilon(q)}}\right) \\
&= \int_{-\pi}^{\pi}\frac{dq}{2\pi}\left(\frac{\epsilon(q)^2e^{-\beta\epsilon(q)}}{k_B^2T^2(1+e^{-\beta\epsilon(q)})}+\frac{\epsilon(q)e^{-\beta\epsilon(q)}}{k_B^2T^2}\frac{(-\epsilon(q))}{(1+e^{-\beta\epsilon(q)})^2}\right) \\
&= \frac{1}{k_B^2T^2}\int_{-\pi}^{\pi}\frac{dq}{2\pi}\frac{\epsilon(q)^2e^{-\beta\epsilon(q)}}{1+e^{-\beta\epsilon(q)}}\left(\frac{e^{\beta\epsilon(q)}}{1+e^{\beta\epsilon(q)}}\right) \\
&= \frac{1}{k_B^2T^2}\int_{-\pi}^{\pi}\frac{dq}{2\pi}\frac{\epsilon(q)^2e^{-\beta\epsilon(q)}}{(1+e^{-\beta\epsilon(q)})^2}.
\end{aligned} \tag{1-37}$$

The magnetization per spin is obtained from the free energy as follows

$$\begin{aligned}
\mathcal{M} &= -\frac{\partial\mathcal{F}}{\partial h} \\
&= -\frac{\partial}{\partial h}\left(-h-k_BT\int_{-\pi}^{\pi}\frac{dq}{2\pi}\ln(1+e^{-2h/T}e^{J\cos q/T})\right) \\
&= 1+k_BT\int_{-\pi}^{\pi}\frac{dq}{2\pi}\frac{e^{-2h\beta}e^{J\beta\cos q}(-2\beta)}{1+e^{-2h\beta}e^{J\beta\cos q}} \\
&= 1-\int_{-\pi}^{\pi}\frac{dq}{\pi}\frac{e^{J\beta\cos q}}{e^{2h\beta}+e^{J\beta\cos q}}.
\end{aligned} \tag{1-38}$$

Finally, the susceptibility per spin is obtained from the magnetization as follows

$$\begin{aligned}
\mathcal{X} &= \frac{\partial\mathcal{M}}{\partial h} \\
&= \frac{\partial}{\partial h}\left(1-\int_{-\pi}^{\pi}\frac{dq}{\pi}\frac{e^{J\beta\cos q}}{e^{2h\beta}+e^{J\beta\cos q}}\right) \\
&= \frac{2}{\pi K_bT}\int_{-\pi}^{\pi}dq\frac{e^{J\beta\cos q}}{(e^{2h\beta}+e^{J\cos q\beta})^2}.
\end{aligned} \tag{1-39}$$

Chapter 2

Emptiness Formation Probability (EFP) $P(n)$ as a Toeplitz determinant

In this chapter, we define one correlation function which allow us to calculate the domain length distribution in the XX model: The Emptiness Formation Probability EFP, $P(n)$. For both cases, zero and finite temperature we show a representation of the EFP in terms of the fermion operators and evaluate the corresponding expression using the Wick's theorem, showing that $P(n)$ can be represented as a Toeplitz determinant. Finally, we reproduce reported results for the asymptotic behavior of $P(n)$ for small and large values of n.

2.1 EFP $P(n)$ at zero temperature

In order to define the EFP first we consider the projection operator $\hat{P}_j$ given by

$$\hat{P}_j = \hat{S}_j^z + \frac{\hat{I}}{2}, \tag{2-1}$$

where the action of the operator $\hat{P}_j$ over an eigenstate of $\hat{S}_j^z$ is given by

$$\hat{P}_j \left|\cdots\uparrow\cdots\right\rangle = \left|\cdots\uparrow\cdots\right\rangle, \quad \text{and} \quad \hat{P}_j \left|\cdots\downarrow\cdots\right\rangle = 0. \tag{2-2}$$

Note that $\hat{P}_j$ projects an arbitrary state on a spin-up state at site number j . At $T = 0$, the distribution $P(n)$ is given by the ground state average of the product of projection operators over n consecutive lattice sites. Thus, $P(n)$ can be written as follows

$$P(n) = \left\langle GS \left| \prod_{j=1}^{n} \left(\hat{S}_j^z + \frac{\hat{I}}{2} \right) \right| GS \right\rangle. \tag{2-3}$$

Consequently, for a spin-1/2 system the Eq. (2-3) gives the probability of finding n adjacent spins up in the antiferromagnetic vacuum [18], where n is an integer number.

The expression that describes the correlation function for the equivalent spinless free fermion system is easy to calculate since S^z is related to the fermionic operators by Eq. (1-19). Then, in terms of the fermionic operators $P(n)$ is given by

$$P(n) = \left\langle GS \left| \prod_{j=1}^{n} \hat{c}_j \hat{c}_j^\dagger \right| GS \right\rangle . \tag{2-4}$$

The correlation function (2-4) can be written as a determinant by using the Wick's theorem [17]. Then, the Eq. (2-4) transforms as follows

$$P(n) = \det \left[\left\langle GS \left| \hat{c}_l \hat{c}_m^\dagger \right| GS \right\rangle \right]_{l,m=1}^{n} . \tag{2-5}$$

To evaluate the determinant, first at all, we have to calculate the expectation value of the product of fermionic operators $\hat{c}_l \hat{c}_m^\dagger$. To do that, note that the fermion operators can be rewritten using the Fourier transform (1-21) obtaining

$$\hat{c}_l \hat{c}_m^\dagger = \frac{1}{N} \sum_{q,q'=1}^{N} \hat{C}_q \hat{C}_{q'}^\dagger e^{i(lq - mq')}. \tag{2-6}$$

The sum of Eq. (2-6) simplifies since when applying the operators over the ket $|GS\rangle$ only remains the states outside of the Fermi's sphere. Also the discrete sum in Eq. (2-6) converges to an integral [1], which integration limits are given by the Fermi radius k_f. Therefore, $P(n)$ can be written as

$$P(n) = \det \left[\frac{1}{2\pi} \int_{k_f}^{2\pi - k_f} e^{i(l-m)q} dq \right]_{l,m=1}^{n} , \tag{2-7}$$

It is well know that the Toeplitz determinant is related to the spacing distribution between level in the random matrices theory. Specifically, the function $A_2(\alpha)$ for the Dyson's circular ensemble of $n \times n$ unitary matrices is identical to eq. (2-7) with the correspondence $k_f = \alpha$. In random matrix theory, $A_2(\alpha)$ is the probability that an interval, of the unit circle, of length 2α contains no eigenvalues [41].

2.1.1 Representation as a Toeplitz determinant

The integral given by Eq. (2-7) depends on the difference between the index l and m, then, it is possible to define a function $a_{l,m} \equiv \tilde{a}_{l-m}$ as follows

$$a_{lm} = \frac{1}{2\pi} \int_{k_f}^{2\pi - k_f} e^{i(l-m)q} dq \equiv \tilde{a}_{l-m}. \tag{2-8}$$

In this way, $\tilde{a}_{l-m}$ is a matrix element that depends on the difference between its index. All matrices whose elements satisfy this property are called as Toeplitz matrices, and the determinant of such matrix is called Toeplitz determinant. For this kind of matrices, the determinant has the form

[1] As usual, for $N \to \infty$ we have $1/N \sum_q \to 1/(2\pi) \int dq$.

$$\det\left[a_{lm}\right]_{l,m=1}^{n} = \begin{pmatrix} a_0 & a_{-1} & & \cdots & & a_{1-n} \\ a_1 & a_0 & a_{-1} & & & \\ & a_1 & a_0 & \ddots & & \\ \vdots & & \ddots & \ddots & \ddots & \\ & & & \ddots & \ddots & a_{-1} \\ a_{n-1} & & & & a_1 & a_0 \end{pmatrix}, \tag{2-9}$$

then, $a_{l,m} = a_{l+1,m+1} \equiv \tilde{a}_{l-m}$, so was demonstrated that is a Toeplitz matrix.

2.1.2 Evaluation of $P(n)$

Evaluating the determinant of a matrix is an operation that computationally will cost more as the matrix size increases, simplify the expression to evaluate will reduce the computational cost of the entire process. Then, note that the integral in eq. (2-7) can be easily evaluated as follows

$$\begin{aligned} P(n) &= \det\left[\frac{1}{2\pi}\int_{k_f}^{2\pi-k_f} e^{i(l-m)q}dq\right]_{l,m=1}^{n} \qquad (2\text{-}10) \\ &= \det\left[\frac{1}{2\pi}\left(\frac{1}{i(l-m)}e^{i(l-m)q}\right)\Big|_{k_f}^{2\pi-k_f}\right]_{l,m=1}^{n} \\ &= \det\left[\frac{1}{2\pi i(l-m)}\left(e^{i(l-m)(2\pi-k_f)} - e^{-i(l-m)k_f}\right)\right]_{l,m=1}^{n} \\ &= \det\left[\frac{1}{2\pi i(l-m)}\left(e^{i(l-m)k_f} - e^{-i(l-m)k_f}\right)\right]_{l,m=1}^{n} \\ &= \det\left[\frac{\sin\left((l-m)k_f\right)}{\pi(l-m)}\right]_{l,m=1}^{n}. \qquad (2\text{-}11) \end{aligned}$$

The evaluation of the expression inside the brackets leads to

$$\left[\frac{1}{\pi(l-m)}\sin((l-m)k_f)\right]_{l,m=1}^{n} = \begin{cases} \dfrac{k_f}{\pi}, & l = m \\ \dfrac{\sin((l-m)k_f)}{\pi(l-m)}, & l \neq m \end{cases} \tag{2-12}$$

Finally, the explicit form of the determinant is

$$\det\left[a_{lm}\right]_{l,m=1}^{n} = \begin{pmatrix} \frac{k_f}{\pi} & \frac{\sin k_f}{\pi} & & \cdots & & \frac{\sin(1-m)k_f}{\pi(1-m)} \\ \frac{\sin k_f}{\pi} & \frac{k_f}{\pi} & \frac{\sin k_f}{\pi} & & & \\ & \frac{\sin k_f}{\pi} & \frac{k_f}{\pi} & \ddots & & \\ \vdots & & \ddots & \ddots & \ddots & \\ & & & \ddots & \ddots & \frac{\sin k_f}{\pi} \\ \frac{\sin(l-1)k_f}{\pi(l-1)} & & & & \frac{\sin k_f}{\pi} & \frac{k_f}{\pi} \end{pmatrix} \tag{2-13}$$

2.1.3 Asymptotics of Toeplitz determinants

In mathematics, the properties of the determinants have been a widely subject of study over the years for different reasons, and the Toeplitz determinants are not an exception. There are many works about their properties, especially in the literature about random matrices. Thus, we can use the known results about the asymptotic behavior of Toeplitz determinants. For a more complete explanation and to see the complete proof of the following theorems, see [41].

Theorem. If $f(\theta)$ is a positive function over $0 \leq \theta \leq 2\pi$, its derivative satisfies a Lipschitz condition and $F_N(f)$ is a $N \times N$ Toeplitz determinant.

$$F_N(f) = \det\left[\frac{1}{2\pi}\int_0^{2\pi} f(\theta)e^{i(j-k)\theta}d\theta\right]_{j,k=1,\ldots,N} \tag{2-14}$$

Then, as $N \to \infty$

$$\log F_N(f) \approx N\, f_0 + \frac{1}{4}\sum_{k=1}^{\infty} k\, f_k f_{-k} + O(1) \tag{2-15}$$

where f_k is the k-th Fourier coefficient of $\log f(\theta)$

$$\log f(\theta) = \sum_{k=-\infty}^{\infty} f_k\, e^{ik\theta}. \tag{2-16}$$

In 1971, Widom extended this theorem for functions $f(\theta)$, which are positive only on an arc of the unit circle [42].

Theorem. Let $f(\theta) = 1$, if $\alpha \leq \theta \leq 2\pi$, and $f(\theta) = 0$ if either $\theta < \alpha$ or $\theta > 2\pi - \alpha$. Then, as $N \to \infty$.

$$\log F_N(f) \approx N^2 \log\cos\frac{\alpha}{2} - \frac{1}{4}\log\left(N\sin\frac{\alpha}{2}\right) + \frac{1}{12}\log 2 + 3\zeta'(-1) \tag{2-17}$$

where $\zeta'(z)$ is the derivative of the Riemann zeta function.

2.1.4 Asymptotic behavior of $P(n)$ at $T = 0$

Let us first assume that h takes some moderate values, i.e., $|h| < h_c$. Then from Widom's theorem for the Toeplitz determinant we have

$$\ln P(n) = n^2 \ln\cos\frac{k_f}{2} - \frac{1}{4}\ln\left(n\sin\frac{k_f}{2}\right) + \frac{1}{12}\ln 2 + 3\zeta'(-1) + o(1), \tag{2-18}$$

which can be rewritten as

$$P(n) \simeq 2^{\frac{1}{12}} e^{3\zeta^{-1}(-1)} \left(\sin^2\left(\frac{kf}{2}\right)\right)^{-1/4} n^{-1/4} \left(\cos^2\left(\frac{kf}{2}\right)\right)^{n^2}, \quad (n \to \infty) \tag{2-19}$$

where $\zeta'(-1) = -0.165421....$ The Eq. (2-19) can be written in terms of the external magnetic field h taking into account that

$$\sin^2\left(\frac{k_f}{2}\right) = \frac{1 - 2h/J}{2} \quad \text{and} \quad \cos^2\left(\frac{k_f}{2}\right) = \frac{1 + 2h/J}{2}.$$

Finally, the Eq. (2-19) takes the form

$$P(n) \simeq 2^{\frac{1}{12}} e^{3\zeta^{-1}(-1)} \left(\frac{1 - 2h/J}{2}\right)^{-1/8} n^{-1/4} \left(\frac{1 + 2h/J}{2}\right)^{n^2/2}, \tag{2-20}$$

from where we conclude that $P(n)$ decays like a Gaussian.

Observe that the pre-factor diverges as h gets closer to the critical value i.e., $h \to h_c = J/2$. There the asymptotic formula may not be adequate. For this region, as k_f is very small, we can expand the determinant with respect to k_f as follows [17]

$$P(n) = 1 - \frac{k_f}{\pi}n + \frac{k_f^4}{36\pi^2}n^2(n^2-1) - \frac{k_f^6}{675}n^2(n^2-1)\left(n^2 - \frac{3}{2}\right) + \cdots \tag{2-21}$$

2.2 $P(n)$ at finite temperature

At finite temperature, the procedure is very similar to the zero-temperature case. However, for $T > 0$ the statistical information of the system is given by the density operator which reduces to the identity operator for zero temperature (pure state). Therefore, for finite temperature, $P(n)$ is given by

$$\begin{aligned} P(n) &\equiv \frac{Tr\left(e^{-\beta\hat{\mathcal{H}}}\prod_{j=1}^{n}\left(\hat{S}_j^z + \frac{1}{2}\right)\right)}{Tr(e^{-\beta\hat{\mathcal{H}}})} \\ &= \left\langle \prod_{j=1}^{n}\left(\hat{S}_j^z + \frac{1}{2}\right)\right\rangle_T \\ &= \left\langle \prod_{j=1}^{n}\left(\hat{c}_l\hat{c}_m^\dagger\right)\right\rangle_T. \end{aligned} \tag{2-22}$$

Using the Bloch-de Dominicis theorem which is an extension of the Wick's theorem for finite temperature, we have [17]

$$P(n) \quad = \quad \det\left[\left\langle \hat{c}_l \hat{c}_m^\dagger \right\rangle_T\right]_{l,m=1}^{n}, \tag{2-23}$$

where the $\left\langle \hat{c}_l \hat{c}_m^\dagger \right\rangle_T$ must be evaluated according to the density operator function of the system

$$P(n) \quad = \quad \det\left[\frac{1}{2\pi}\int_0^{2\pi} e^{i(l-m)q}\rho(q)dq\right]_{l,m=1}^{n}. \tag{2-24}$$

.

Given that we are dealing with a fermionic system, the density function $\rho(q)$ is related to the Fermi-Dirac distribution n_q according to

$$\rho(q) = \sum_q e^{-\epsilon(q)/T} = \frac{1}{1+e^{-\epsilon(q)/T}} = 1 - n_q, \quad \text{and} \quad \epsilon(q) = 2h - J\cos q. \tag{2-25}$$

The asymptotic behavior of $P(n)$ can be determined by using Szegö's v theorem to the Toeplitz determinant, for a large explanation and a rigorous proof of the theorem see chapter 10 of Ref. [43]. Using this theorem, it is possible to write

$$\ln P(n) = n\rho_0 + \sum_{k=1}^{\infty} k\rho_k\rho_{-k} + o(1), \quad \text{where} \quad \ln\rho_q = \sum_{k=-\infty}^{\infty} \rho e^{ikq}. \tag{2-26}$$

Particularly, we have

$$\rho_0 = -\frac{1}{2\pi}\int_0^{2\pi} \ln\left(1+e^{-\epsilon(q)/T}\right) dq. \tag{2-27}$$

Then, we conclude that at finite temperature $P(n)$ decays exponentially according to

$$P(n) \simeq c(T,h)e^{-n/\xi}. \tag{2-28}$$

In Eq. (2-28) the inverse of the correlation length ξ^{-1} and the prefactor $c(T,h)$ are given by

$$\xi^{-1} = -\frac{f(T,h)+h}{T} = \frac{1}{2\pi}\int_0^{2\pi} \ln\left[1+e^{\frac{J\cos q - 2h}{T}}\right] dq, \tag{2-29}$$

and

$$c(T,h) \quad = \quad \sum_{k=1}^{\infty} k\,\rho_k\rho_{-k} = \frac{1}{8}\int_0^{2\pi}\frac{dq}{2\pi}\int_0^{2\pi}\frac{d\tilde{q}}{2\pi}\left(\frac{\ln\rho(q) - \ln\rho(q)}{\sin\frac{1}{2}(q-\tilde{q})}\right)^2. \tag{2-30}$$

It is possible to probe that the inverse of the correlation length diverges when $T=0$ if $|h| < h_c$. Therefore, ξ approaches to zero in the low temperature limit, indicating the crossover between the exponential and a Gaussian decay.

Chapter 3

Spacing distributions using the IPDF method

In this chapter, we introduce the principal concepts about the IPDF method and define the n-th spacing-distribution function p_n^m. The IPDF method allow one to write p_n^0 in terms of the distribution $P(n)$ that was introduced in chapter 2. Later, we extend the method to calculate the second spacing-distribution p_n^1. Finally, we present the generalized Wigner surmise (GWS) for spacing distributions in order to compare the exact distributions calculated using the IPDF method.

3.1 The IPDF method

The Interparticle distribution function (IPDF) method was originally introduced in 1988 by ben-Avraham for the solution of the diffusion-limited coalescence process $A + A \to A$ in one dimension [44]. Some examples of the use of the IPDF method can be found in [23–25]. The following derivation of the IPDF method can be found in chapter 15 of [26] along with some applications to simple reaction-diffusion systems.

In the fermion equivalent system p_n^m is the probability of have one fermion in $l = 0$ and another one in $l = n$ with the condition that there are m fermions between them. Consequently, $p_n^0 = \mathcal{P}(\bullet\overbrace{\circ\cdots\circ}^{n}\bullet)$ is the probability to find the following configuration

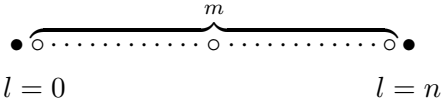

In the spin system p_n^0 corresponds to the domain length distribution. Let $\mathcal{P}(\bullet\overbrace{\circ\cdots\circ}^{m-1}\bullet\overbrace{\circ\cdots\circ\cdots\circ}^{n-m+1}\bullet)$ the probability of the following configuration

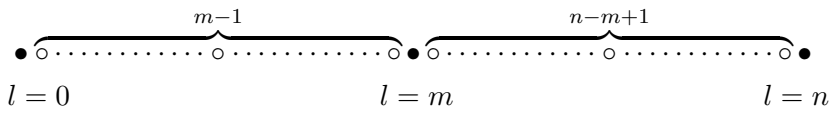

Following its definition, p_n^1 can be written as

$$\begin{aligned} p_n^1 &= \sum_m \mathcal{P}(\bullet \overbrace{\circ\cdots\circ}^{m-1} \bullet \overbrace{\circ\cdots\circ\cdots\circ}^{n-m+1} \bullet) \\ &= \sum_m \mathcal{P}(\downarrow \overbrace{\uparrow\cdots\uparrow}^{m-1} \downarrow \overbrace{\uparrow\cdots\uparrow\cdots\uparrow}^{n-m+1} \downarrow) \end{aligned} \tag{3-1}$$

In the equivalent spin system p_n^1 is the probability to find two consecutive up domains with total length $n-1$ separated by a single spin down. In the following sections we calculate analytically p_n^0 and p_n^1 using the IPDF method.

3.2 p_n^0 distribution

Consider a one-dimensional lattice in which each lattice site can be either empty ($\circ$) or occupied ($\bullet$) by a single particle. In this way, for an arbitrary lattice site there are two possible states, empty or occupied, which probabilities must satisfy the following equation

$$\mathcal{P}(\bullet) + \mathcal{P}(\circ) = 1, \tag{3-2}$$

The Eq. (3-2) is no more than the axiom of the conservation of the probability. Consider two consecutive sites, regardless of what is in the left or right, the probabilities of the resulting configurations satisfy

$$\mathcal{P}(\circ\circ) + \mathcal{P}(\circ\bullet) + \mathcal{P}(\bullet\circ) + \mathcal{P}(\bullet\bullet) = 1. \tag{3-3}$$

If the system is isotropic then, the third and fourth terms of Eq. (3-3) are equal, i.e., $\mathcal{P}(\circ\bullet) = \mathcal{P}(\bullet\circ)$. On the other hand, in Chapter 2, we define $P(n) \equiv P_n$ as the probability that a randomly chosen an empty segment of n consecutive sites, i.e., containing no particles. Taking into account this definition and the isotropy condition, we get that the Eq. (3-3) transforms as follows

$$\mathcal{P}(\bullet\bullet) + 2\mathcal{P}(\bullet\circ) + P_2 = 1 \tag{3-4}$$

Now let's consider two consecutive sites with the one at the left empty. The probabilities of the respective configurations satisfy

$$\begin{aligned} \mathcal{P}(\circ\bullet) + \mathcal{P}(\circ\circ) &= \mathcal{P}(\circ) \\ \mathcal{P}(\circ\bullet) &= P_1 - P_2 \end{aligned} \tag{3-5}$$

Thus, replacing Eq. (3-5) into Eq. (3-4) we get

$$\begin{aligned} \mathcal{P}(\bullet\bullet) + 2(P_1 - P_2) + P_2 &= 1 \\ \mathcal{P}(\bullet\bullet) &= 1 - 2P_1 + P_2. \end{aligned} \tag{3-6}$$

Note that in above equation we have written the probabilities associated to the configurations of two consecutive sites in terms of probabilities known a priori, (P_n). Now, we consider all the sequences of $n+1$ sites with the $n-1$ inner sites empty. The configurations and their respective probabilities are shown below

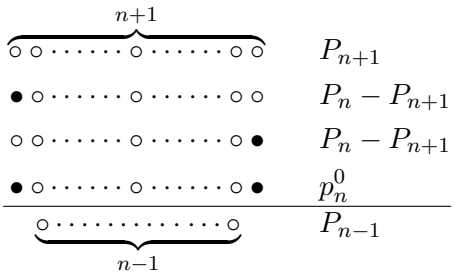

These probabilities are related according to

$$P_{n+1} + 2(P_n - P_{n+1}) + p_n^0 = P_{n-1}, \tag{3-7}$$

Therefore, the domain length distribution can be calculated from the EFP defined in Chapter 2 by using

$$p_n^0 = P_{n+1} + P_{n-1} - 2P_n. \tag{3-8}$$

It is very illustrative to show that expressions derived in this section can be also obtained by using the fermionic formalism. In order to do that, note that the Eq. (3-8) can be written as follows

$$p_n^0 = \left\langle \hat{c}_0^\dagger \hat{c}_0 \left(\prod_{l=1}^{n-1} \hat{b}_l^\dagger \hat{b}_l \right) \hat{c}_n^\dagger \hat{c}_n \right\rangle. \tag{3-9}$$

To simply the notation we define the operator $\hat{O} = \prod_{l=1}^{n-1} \hat{b}_l^\dagger \hat{b}_l$ and remember the definition of the EFP $P_n = \left\langle \prod_{l=1}^{n} \hat{b}_l^\dagger \hat{b}_l \right\rangle$. Note that p_n^0 can be studied in terms of the formation of occupied states $\hat{c}_j^\dagger \hat{c}_j$ or empty sites $\hat{b}_j^\dagger \hat{b}_j$ which satisfy $\hat{c}_j^\dagger \hat{c}_j = 1 - \hat{b}_j^\dagger \hat{b}_j$. Thus, using the hole operators the Eq. (3-9) transforms as follows

$$
\begin{aligned}
p_n^0 &= \left\langle (1-\hat{b}_0^\dagger\hat{b}_0)\hat{O}(1-\hat{b}_n^\dagger\hat{b}_n)\right\rangle \\
&= \left\langle (\hat{O}-\hat{b}_0^\dagger\hat{b}_0\hat{O})(1-\hat{b}_n^\dagger\hat{b}_n)\right\rangle \\
&= \left\langle \prod_{l=1}^{n-1}\hat{b}_l^\dagger\hat{b}_l\right\rangle - \left\langle \prod_{l=1}^{n}\hat{b}_l^\dagger\hat{b}_l\right\rangle - \left\langle \prod_{l=0}^{n-1}\hat{b}_l^\dagger\hat{b}_l\right\rangle + \left\langle \prod_{l=0}^{n}\hat{b}_l^\dagger\hat{b}_l\right\rangle \\
&= P_{n-1} - 2P_n + P_{n+1}, \qquad (3\text{-}10)
\end{aligned}
$$

where we must consider that the second and third terms in the penultimate line represent the same probability. Clearly, we have recovered Eq. (3-8) as expected.

3.3 p_n^1 distribution

In terms of the fermionic operators the distribution P_n^1 can be written as follows

$$
P_n^1 = \sum_{m=1}^{n-1}\left\langle \hat{c}_0^\dagger\hat{c}_0\left(\prod_{l=1}^{m-1}\hat{b}_l^\dagger\hat{b}_l\right)\hat{c}_m^\dagger\hat{c}_m\left(\prod_{l=m+1}^{n-1}\hat{b}_l^\dagger\hat{b}_l\right)\hat{c}_n^\dagger\hat{c}_n\right\rangle, \qquad (3\text{-}11)
$$

As illustrated in Eq. (3-1), we must sum over m to consider all possible configurations with a fermion at $l=0$ and another one at $l=n$ with an additional fermion in between. As in previous section, it is convenient to express the equation in terms of the hole operators as follows

$$
\begin{aligned}
P_n^1 &= \sum_{m=1}^{n-1}\left\langle (1-\hat{b}_0^\dagger\hat{b}_0)\hat{O}_1(1-\hat{b}_m^\dagger\hat{b}_m)\hat{O}_2(1-\hat{b}_n^\dagger\hat{b}_n)\right\rangle \\
&= \sum_{m=1}^{n-1}\left\langle (\hat{O}_1-\hat{b}_0^\dagger\hat{b}_0\hat{O}_1-\hat{O}_1\hat{b}_m^\dagger\hat{b}_m+\hat{b}_0^\dagger\hat{b}_0\hat{O}_1\hat{b}_m^\dagger\hat{b}_m)(\hat{O}_2-\hat{O}_2\hat{b}_n^\dagger\hat{b}_n)\right\rangle \\
&= \sum_{m=1}^{n-1}\left\langle \hat{O}_1\hat{O}_2-\hat{b}_0^\dagger\hat{b}_0\hat{O}_1\hat{O}_2-\hat{O}_1\hat{b}_m^\dagger\hat{b}_m\hat{O}_2+\hat{b}_0^\dagger\hat{b}_0\hat{O}_1\hat{b}_m^\dagger\hat{b}_m\hat{O}_2\right\rangle \\
&\quad -\sum_{m=1}^{n-1}\left\langle \hat{b}_0^\dagger\hat{b}_0\hat{O}_1\hat{O}_2\hat{b}_n^\dagger\hat{b}_n-\hat{O}_1\hat{b}_m^\dagger\hat{b}_m\hat{O}_2\hat{b}_n^\dagger\hat{b}_n+\hat{b}_0^\dagger\hat{b}_0\hat{O}_1\hat{b}_m^\dagger\hat{b}_m\hat{O}_2\hat{b}_n^\dagger\hat{b}_n\right\rangle. \qquad (3\text{-}12)
\end{aligned}
$$

We define $P_{n,m}$ as the probability of having the following configuration

$$
\begin{array}{ccccccccc}
\circ & \cdots\cdots\cdots & \circ & & \circ & \cdots\cdots\cdots & \circ \\
l=0 & & l=m-1 & l=m & l=m+1 & & l=n
\end{array} \qquad (3\text{-}13)
$$

This is nothing more that the probability to have two consecutive empty intervals, one from $l = 0$ to $l = m - 1$ and the other one from $l = m + 1$ to $l = n$, regardless of what we have at the position $l = m$. Expanding the Eq. (3-12) we found

$$
\begin{aligned}
p_n^1 \;=\; & \sum_{m=1}^{n-1} \Bigg[\underbrace{\left\langle \prod_{l=1}^{m-1} \hat{b}_l^\dagger \hat{b}_l \prod_{l=m+1}^{n-1} \hat{b}_l^\dagger \hat{b}_l \right\rangle}_{(1)} - \underbrace{\left\langle \prod_{l=0}^{m-1} \hat{b}_l^\dagger \hat{b}_l \prod_{l=m+1}^{n-1} \hat{b}_l^\dagger \hat{b}_l \right\rangle}_{(2)} - \underbrace{\left\langle \prod_{l=1}^{n-1} \hat{b}_l^\dagger \hat{b}_l \right\rangle}_{(3)} + \underbrace{\left\langle \prod_{l=0}^{n-1} \hat{b}_l^\dagger \hat{b}_l \right\rangle}_{(4)} \Bigg] \\
& - \sum_{m=1}^{n-1} \Bigg[\underbrace{\left\langle \prod_{l=1}^{m-1} \hat{b}_l^\dagger \hat{b}_l \prod_{l=m+1}^{n} \hat{b}_l^\dagger \hat{b}_l \right\rangle}_{(5)} - \underbrace{\left\langle \prod_{l=0}^{m-1} \hat{b}_l^\dagger \hat{b}_l \prod_{l=m+1}^{n} \hat{b}_l^\dagger \hat{b}_l \right\rangle}_{(6)} - \underbrace{\left\langle \prod_{l=1}^{n} \hat{b}_l^\dagger \hat{b}_l \right\rangle}_{(7)} + \underbrace{\left\langle \prod_{l=0}^{n} \hat{b}_l^\dagger \hat{b}_l \right\rangle}_{(8)} \Bigg] ,
\end{aligned}
\tag{3-14}
$$

Expressed in this way, it is easy to see in each term where to hole is located, so the Eq. (3-14) takes the form

$$
p_n^1 = \sum_m \left(P_{n-2,m-1} - P_{n-1,m} - P_{n-1,m-1} + P_{n,m} - p_n^0 \right) , \tag{3-15}
$$

where p_n^0 is given by the Eq. (3-8). Now, we will show that Eq. (3-15) agrees with the configurations described graphically in the previous section. In the Table **3-1** we present a graphic representation of each term of Eq. (3-14). According to the rules of the IPDF method, the probability of those configurations are related according to

$$
\begin{aligned}
P(\mathcal{C}_1) - P(\mathcal{C}_2) &= P(\mathcal{C}_9) && \text{(3-16)} \\
P(\mathcal{C}_3) - P(\mathcal{C}_4) &= P(\mathcal{C}_{10}) && \text{(3-17)} \\
P(\mathcal{C}_5) - P(\mathcal{C}_6) &= P(\mathcal{C}_{11}) && \text{(3-18)} \\
P(\mathcal{C}_7) - P(\mathcal{C}_8) &= P(\mathcal{C}_{12}). && \text{(3-19)}
\end{aligned}
$$

The graphic representation of the elements $P(\mathcal{C}_9)$, $P(\mathcal{C}_{10})$, $P(\mathcal{C}_{11})$ and $P(\mathcal{C}_{12})$ are given in Table **3-2**, from where we can conclude that

$$
\begin{aligned}
P(\mathcal{C}_9) - P(\mathcal{C}_{10}) &= P(\mathcal{C}_{13}) && \text{(3-20)} \\
P(\mathcal{C}_{11}) - P(\mathcal{C}_{12}) &= P(\mathcal{C}_{14}), && \text{(3-21)}
\end{aligned}
$$

In the same way, from Tables **3-3** and **3-4** we found

$$
P(\mathcal{C}_{13}) - P(\mathcal{C}_{14}) = P(\mathcal{C}_{15}). \tag{3-22}
$$

Finally, P_n^1 is given by $P_n^1 = \sum_{m=1}^{n-1} P(\mathcal{C}_{15})$.

probability	sign	0	1		$m-1$	m	$m+1$		$n-1$	n
$P(\mathcal{C}_1)$	+		○	·····	○		○	·····	○	
$P(\mathcal{C}_2)$	-	○	○	·····	○		○	·····	○	
$P(\mathcal{C}_3)$	-		○	·····	○	○	○	·····	○	
$P(\mathcal{C}_4)$	+	○	○	·····	○	○	○	·····	○	
$P(\mathcal{C}_5)$	-		○	·····	○		○	·····	○	○
$P(\mathcal{C}_6)$	+	○	○	·····	○	○	○	·····	○	○
$P(\mathcal{C}_7)$	+		○	·····	○	○	○	·····	○	○
$P(\mathcal{C}_8)$	-	○	○	·····	○	○	○	·····	○	○

Table **3-1**: Graphic representation of the spacing-distributions given by probabilities $\mathcal{P}(\mathcal{C}_1)$ to $\mathcal{P}(\mathcal{C}_8)$ for IPDF calculations.

probability	sign	0	1		$m-1$	m	$m+1$		$n-1$	n
$P(\mathcal{C}_9)$	+	●	○	·····	○		○	·····	○	
$P(\mathcal{C}_{10})$	-	●	○	·····	○	○	○	·····	○	
$P(\mathcal{C}_{11})$	-	●	○	·····	○		○	·····	○	○
$P(\mathcal{C}_{12})$	+	●	○	·····	○	○	○	·····	○	○

Table **3-2**: Graphic representation of the spacing-distributions given by probabilities $\mathcal{P}(\mathcal{C}_9)$ to $\mathcal{P}(\mathcal{C}_{12})$ for IPDF calculations.

probability	sign	0	1		$m-1$	m	$m+1$		$n-1$	n
$P(\mathcal{C}_{13})$	+	●	○	·····	○	●	○	·····	○	
$P(\mathcal{C}_{14})$	-	●	○	·····	○	●	○	·····	○	●

Table **3-3**: Graphic representation of the spacing-distributions given by probabilities $\mathcal{P}(\mathcal{C}_{13})$ and $\mathcal{P}(\mathcal{C}_{14})$ for IPDF calculations.

probability	sign	0	1		$m-1$	m	$m+1$		$n-1$	n
$P(\mathcal{C}_{15})$	+	●	○	·····	○	●	○	·····	○	●

Table **3-4**: Graphic representation of the spacing-distributions given by probability $\mathcal{P}(\mathcal{C}_{15})$ for IPDF calculations.

Chapter 4

Stochastic Series Expansion Quantum Monte Carlo (SSE QMC)

In this chapter we present the main concepts associated to the implementation of the Quantum Monte Carlo (QMC) method based in the called Stochastic Series Expansion (SSE) in detail. First, we explain how to apply this algorithm to the pure Heisenberg model (with zero magnetic field), and then, extend the procedure to the case of non-zero magnetic field. Finally, we explain the most important details for the code implementation of the algorithm for the isotropic spin-1/2 Heisenberg model with magnetic field.

4.1 The Quantum Monte Carlo Method

Since Feynman proposed the path integral formulation for quantum statistical mechanics [45], there has been a lot of progress in the development of QMC methods. For example, the called "*world line methods*", which are based on the path integral formulation in imaginary time (τ), have been applied successfully to spin systems and related lattice models [46]. This procedure is known as Suzuki-Trotter decomposition [47, 48]. There are also exact algorithms operating directly in the imaginary continuum time [49].

In the decade of 1960s Handscomb developed an approximation-free method for the Heisenberg ferromagnets based on the power-series expansion of $e^{-\beta\mathcal{H}}$ and exactly computable traces of products operators [50]. This method was applied first Heisenberg ferromagnets [51] and later was generalized to the Heisenberg antiferromagnet [52, 53], including spin-1/2 systems [54, 55]. The power-series approach to QMC calculations was updated by Sandvik with the introduction of a more general and exact stochastic series expansion SSE formulation. In Sandvik's approach, the traces are also sampled showing clearly how closely the discrete power series is related to the path integral in continuous imaginary time [3]. The spin configurations for some models, such as the Heisenberg, can be sampled efficiently by using loop-cluster updates [56]. This sampling method is a generalization of the classical Swendsen-Wang cluster algorithm for quantum systems [57]. However, the direct loops have an even wider applicability, e.g., for the Heisenberg spin chain in the presence of external fields.

4.2 SSE for the partition function

In the SSE method, the Hamiltonian is decomposed into two terms, the first includes the diagonal part of the Hamiltonian and the second the non-diagonal one. The equilibrium state is obtained through a fictional evolution (imaginary-time evolution) in which the operators are updated by independent inserting and removing diagonal and non-diagonal operators [58].

In quantum statistical mechanics, we are interested in calculating the expectation value of some operator A at temperature T for a given Hamiltonian $\hat{\mathcal{H}}$ as follows

$$\left\langle \hat{A} \right\rangle = \frac{1}{\mathcal{Z}_N(\beta)} Tr\left(\hat{A} e^{-\beta \hat{\mathcal{H}}} \right), \quad \text{with} \quad \mathcal{Z}_N(\beta) = Tr\left(e^{-\beta \mathcal{H}} \right), \tag{4-1}$$

where we have defined $\mathcal{Z}_N(\beta)$ as the partition function of the system. For simplicity, we will work in units where all constants of nature are set to unity, then, $\beta = 1/T$.

In a spin-1/2 chain $\hat{\mathcal{H}}$ is represented by a $2^N \times 2^N$ matrix. To evaluate this partition function using Monte Carlo, we must write $\mathcal{Z}_N(\beta)$ in terms of higher-dimensional sums. To do that we expand the partition function of Eq. (4-1) in a Taylor series as follows

$$\begin{aligned} \mathcal{Z}_N(\beta) &= \sum_{\alpha_0} \left\langle \alpha_0 \left| e^{-\beta \hat{\mathcal{H}}} \right| \alpha_0 \right\rangle \\ &= \sum_{\alpha_0} \sum_{n=0}^{\infty} \frac{\beta^n}{n!} \left\langle \alpha_0 \left| (-\hat{\mathcal{H}})^n \right| \alpha_0 \right\rangle, \end{aligned} \tag{4-2}$$

since α_j's form a complete basis they must satisfy $\sum_{\alpha_j} |\alpha_j\rangle\langle\alpha_j| = \hat{I}$, inserting this completeness relation in Eq. (4-2) we obtain

$$\mathcal{Z}_N(\beta) = \sum_n \sum_{\{\alpha\}} \frac{(-\beta)^n}{n!} \left\langle \alpha_0 \left| \hat{\mathcal{H}} \right| \alpha_1 \right\rangle \left\langle \alpha_1 \left| \hat{\mathcal{H}} \right| \alpha_2 \right\rangle \cdots \left\langle \alpha_{n-1} \left| \hat{\mathcal{H}} \right| \alpha_0 \right\rangle, \tag{4-3}$$

where the sum over $\{\alpha\}$, i.e. α_0, α_1, α_2,..., α_{n-1}. The equation Eq. (4-3) is a high-dimensional sum in a large space, a perfect candidate to apply the Monte Carlo method.

4.2.1 Importance sampling and weights

Importance sampling is a general technique for estimating the properties of a particular distribution, while only having samples generated from a different distribution than the distribution of interest [59]. The system studied in this chapter is specially well suited to importance sampling since almost all of the terms in the sum will be zero since a matrix element connecting any two states is very likely to be zero-valued, then $\hat{\mathcal{H}}$ is extremely sparse.

The objective is to compute transition probabilities between micro-states using $\mathcal{Z}_N(\beta)$ as the weight of each configuration; to do that, we rewrite $\mathcal{Z}_N(\beta)$ in terms of M operators $\hat{\mathcal{O}}_i$, such as, n of these

operator $\hat{\mathcal{O}}_i$ are local matrix elements of $\hat{\mathcal{H}}$ and the remaining ones $M-n$ are identity operators $\hat{\mathbb{I}}$. So, the Eq. (4-3) transforms as follows

$$\begin{aligned}\mathcal{Z}_N(\beta) &= \sum_{n=0}^{M}\sum_{\{\alpha\}}\frac{(-\beta)^n}{n!}\left(\frac{n!(M-n)!}{M!}\right)\left\langle\alpha_0\left|\hat{\mathcal{O}}_0\right|\alpha_1\right\rangle\left\langle\alpha_1\left|\hat{\mathcal{O}}_2\right|\alpha_2\right\rangle\cdots\left\langle\alpha_{n-1}\left|\hat{\mathcal{O}}_{M-1}\right|\alpha_0\right\rangle \\ &= \sum_{n=0}^{M}\sum_{\{\alpha\}}\frac{(-\beta)^n(M-n)!}{M!}\left\langle\alpha_0\left|\hat{\mathcal{O}}_0\right|\alpha_1\right\rangle\left\langle\alpha_1\left|\hat{\mathcal{O}}_2\right|\alpha_2\right\rangle\cdots\left\langle\alpha_{n-1}\left|\hat{\mathcal{O}}_{M-1}\right|\alpha_0\right\rangle. \qquad (4\text{-}4)\end{aligned}$$

Each term in Eq. (4-4) represents a configuration in the simulation space, which consists of a set of $\{\alpha\}$ with M operators $\hat{\mathcal{O}}_j$. Then, from Eq. (4-4) we can define the weight of a configuration as follows

$$\mathcal{W}(\{\alpha\}) = \frac{(-\beta)^n(M-n)!}{M!}\left\langle\alpha_0\left|\hat{\mathcal{O}}_0\right|\alpha_1\right\rangle\left\langle\alpha_1\left|\hat{\mathcal{O}}_2\right|\alpha_2\right\rangle\cdots\left\langle\alpha_{n-1}\left|\hat{\mathcal{O}}_{M-1}\right|\alpha_0\right\rangle. \qquad (4\text{-}5)$$

Since we are working with a Hamiltonian with pair-wise interaction we can conclude that there is a short list of values of non-zero matrix elements $\langle\alpha_p|\mathcal{H}|\alpha_{p+1}\rangle$, thus, we can rewrite Eq. (4-5) in terms of a short list of non-zero operators types as follows

$$\mathcal{W} = \frac{(-\beta)^n(M-n)!}{M!}\left(\mathcal{W}_1\right)^{n_1}\left(\mathcal{W}_2\right)^{n_2}\left(\mathcal{W}_3\right)^{n_3}\cdots, \quad \text{with} \quad \sum_j n_j = n, \qquad (4\text{-}6)$$

where n_j refers to the number of operators of type j with an associated weight $\mathcal{W}_j$. We must remark that we will never evaluate the weight itself, but the quotient of the weights of closely related configurations, avoiding the issue of evaluating the factorials of large numbers.

4.2.2 The sign problem

The quantum mechanical problem differs from the classical case since every term in the classical partition function is positive and real. Therefore, it is trivial to guarantee that the Monte Carlo weights assigned to each configuration are also positive and real. The same cannot be said for the terms in $\mathcal{Z}_N(\beta)$, some of them will be negative or even possible imaginary. This is known as the sign problem [60] which is almost always present in fermionic systems, except for systems where there is a mapping onto an effective bosonic model. The sign problem is often present also in frustrated spin systems [58, 60].

The sign problem for the SSE method can be seen in Eq. (4-6). Note that, depending on the parity of n the weights $\mathcal{W}_j$ can be positive or negative or even imaginary.

4.3 The Heisenberg Model

As mentioned in previous chapters, we consider the Heisenberg model for the antiferromagnetic case, i.e., $J > 0$, and restrict ourselves to a bipartite lattice. The Hamiltonian is given by

$$\begin{aligned}\hat{\mathcal{H}}_J &= J\sum_{<j,k>}\vec{S}_j\cdot\vec{S}_k \\ &= J\sum_{<j,k>}\left[\hat{S}_j^z\hat{S}_k^z+\frac{1}{2}\left(\hat{S}_j^+\hat{S}_k^-+\hat{S}_j^-\hat{S}_k^+\right)\right],\end{aligned} \tag{4-7}$$

since we are working with a bipartite lattice we need an index to identify the elements of each sublattice, in this way j and k represent the index of the first and second sublattice, respectively, and $< j,k >$ simply denotes that we perform the sum over both sublattices. From the above equation we can see how this Hamiltonian acts on a pair of spins (bonds) in the $\hat{S}^z$ basis. Each matrix element will possess four spins corresponding to the "before" and "after" spins

$$\left\langle \hat{S}_{j,f}^z\hat{S}_{k,f}^z\left|\hat{\mathcal{H}}_J\right|\hat{S}_{j,o}^z\hat{S}_{k,o}^z\right\rangle, \tag{4-8}$$

where $\hat{S}_{j,o}^z$ and $\hat{S}_{j,f}^z$ denote the spin operator before and after the interaction, respectively. There are 2^4 possible combinations of legs of such an operator, but we can immediately discard those that do not conserve the total spin for the $\hat{z}$ axis. The allowed cases of Eq. (4-8) can be easily evaluated using Eq. (1-13), obtaining

$$\left\langle \pm\pm\left|\hat{\mathcal{H}}_J\right|\pm\pm\right\rangle=\frac{J}{4},\quad \left\langle \pm\mp\left|\hat{\mathcal{H}}_J\right|\pm\mp\right\rangle=-\frac{J}{4},\quad \text{and}\quad \left\langle \pm\mp\left|\hat{\mathcal{H}}_J\right|\mp\pm\right\rangle=\frac{J}{2}. \tag{4-9}$$

Here after, we will refer to these local matrix elements as vertices. We obtain that for the Heinsenberg model with zero field there are 6 vertices that preserves the total spin for the $\hat{z}$ axis. They all are real but two of them are negative. As mentioned before, this causes troubles when evaluating the Eq. (4-6), restricting us to take certain values of n so that the Eq. (4-6) be always positive.

4.3.1 The sign problem in the Heisenberg model

In this case, the solution of the sign problem is quite simple, for SSE to work, all vertices of Eq. (4-6) must be smaller than zero, so that the weights of each configuration are guaranteed to be positive or zero. Let's introduce the following term to the Hamiltonian of Eq. (4-7)

$$\begin{aligned}\hat{\mathcal{H}}_{J,n_b} &= \hat{\mathcal{H}}_J-\frac{Jn_b}{4} \\ &= J\sum_{<j,k>}\left(\hat{S}_j^z\hat{S}_k^z-\frac{1}{4}\right)+\frac{J}{2}\sum_{<j,k>}\left(\hat{S}_j^+\hat{S}_k^-+\hat{S}_j^-\hat{S}_k^+\right).\end{aligned} \tag{4-10}$$

Note that the constant does not alters the spectrum, only introduce a shift in the energy that can be removed later. Then, we rotate one the sublattices by π rad about the $\hat{z}$ axis. This has the effect of rotating all the spin operator acting in each lattice site as follows

$$\hat{S}_j^x\to-\hat{S}_j^x,\quad \hat{S}_j^y\to-\hat{S}_j^y,\quad \text{and}\quad \hat{S}_j^z\to-\hat{S}_j^z. \tag{4-11}$$

Then, the ladder operators transform as follows

$$\hat{S}_j^+ \to -\hat{S}_j^+, \quad \text{and} \quad \hat{S}_j^- \to -\hat{S}_j^-. \tag{4-12}$$

Therefore, the Hamiltonian of Eq. (4-10) finally takes the form

$$\hat{\mathcal{H}}_{J,n_b}^{rot(\pi)} = -J \sum_{<j,k>} \left(\frac{1}{4} - \hat{S}_j^z \hat{S}_k^z \right) - \frac{J}{2} \sum_{<j,k>} \left(\hat{S}_j^+ \hat{S}_k^- + \hat{S}_j^- \hat{S}_k^+ \right) \equiv \hat{\mathcal{H}}. \tag{4-13}$$

Now, calculating again the allowed cases of Eq. (4-8), but this time using the Hamiltonian of the Eq. (4-13) we obtain that the vertices of Eq. (4-9) transform as follows

$$\left\langle \pm \pm \left| \hat{\mathcal{H}} \right| \pm \pm \right\rangle = 0, \quad \left\langle \pm \mp \left| \hat{\mathcal{H}} \right| \pm \mp \right\rangle = -\frac{J}{2}, \quad \text{and} \quad \left\langle \pm \mp \left| \hat{\mathcal{H}} \right| \mp \pm \right\rangle = -\frac{J}{2}. \tag{4-14}$$

The added constant set all the diagonal vertices (which involve parallel spins) to 0 and the sub-lattice rotation makes the off-diagonal vertices (which involve antiparallel spins) negative. Now all the non-zero weights all set to be negative, in the Eq. (4-6) results a $(-1)^n$ term that compensates the appearing in the term $(-\beta)^n$. Then, all the non-zero weights will be positive, solving the sign problem.

4.4 SSE for the isotropic spin-1/2 Heisenberg model

There are only two kinds of non-zero operators called diagonal and off-diagonal operators. Then, the Hamiltonian of the system can be decomposed into two terms

$$\hat{\mathcal{H}} = J \sum_b \left(\hat{\mathcal{H}}_{1,b} + \hat{\mathcal{H}}_{2,b} \right), \tag{4-15}$$

where $\hat{\mathcal{H}}_{1,b}$ represents the diagonal terms and $\hat{\mathcal{H}}_{1,b}$ the off-diagonal ones and are given by

$$\hat{\mathcal{H}}_{1,b} = -\frac{1}{4} + \hat{S}_{j(b)}^z \hat{S}_{k(b)}^z \quad \text{and} \quad \hat{\mathcal{H}}_{2,b} = -\frac{1}{2} \left(\hat{S}_{j(b)}^+ \hat{S}_{k(b)}^- + \hat{S}_{j(b)}^- \hat{S}_{k(b)}^+ \right). \tag{4-16}$$

The sum in Eq. (4-15) is not over the lattice sites but over the lattice bonds, b. A bond is the joint of two adjacent lattice points. The dynamics of the system is given by the constant change of the configurations, i.e., the change of the position and the number of diagonal and off-diagonal operators. In the following sections, we will explain the update scheme for both, diagonal, and off-diagonal operators.

We define a propagated state $|\alpha(p)\rangle$ as the stored basis state $|\alpha\rangle = |\alpha(0)\rangle$ propagated by the first p operators in the string as follows

$$|\alpha(p)\rangle = \prod_{j=1}^{p} \hat{\mathcal{H}}_{a(j),b(j)} |\alpha\rangle, \tag{4-17}$$

where $a(j)$ denotes the type of operator and $b(j)$ the bond. We remark that each operator acts on one *timeslice*, the time-slices refers to the fictional expansion, mentioned before. These states are of course also basis states. This is another key aspect of the SSE method; that the operators and basis have to be chosen such that propagating a basis state with an operator string leads to a sequence of single basis states, i.e., there is no branching of configurations (paths) [28].

4.4.1 Sampling and updating scheme

We must discuss how to update the configurations. In Monte Carlo importance sampling, we start from some arbitrary allowed configuration, i.e., with non-zero weight ($\mathcal{W} \neq 0$). From the initial configuration we generate a Markov chain of configurations by making changes (updates) that are accepted or rejected according to some probabilities that are chosen in such way that the detailed balance condition is satisfied. In this way the probability distribution is sampled [2,28]. Using the Metropolis method [61], the probabilities to accept an update from a given configuration is given by

$$P_{accept} = \min\left(\frac{\mathcal{W}_{new}}{\mathcal{W}_{old}}, 1\right). \tag{4-18}$$

The decision of whether to accept the update is made by comparing the probability given in Eq. (4-18) with a random number uniformly distributed $R \in [0, 1)$; If $R > P_{accept}$, the update is rejected and the old configuration is kept. With the Metropolis acceptance probability, Eq. (4-18), the probability of making an update from a current configuration A to a new configuration B must be the same as the probability of making the change to A when the current configuration is B, but this is not always the case when updating an SSE configuration.

Consider two configurations A and B, for which there is an update that can change them into each other. If the probability for selecting B when in A is not the same as selecting A when in B, one can use the following acceptance probability [28]

$$P_{accept}(A \to B) = \min\left(\frac{\mathcal{W}(B)P_{accept}(B \to A)}{\mathcal{W}(A)P_{accept}(A \to B)}, 1\right). \tag{4-19}$$

In the SSE method for the Heisenberg model, there are three types of updates, called *diagonal update*, *single-spin flip*, and *loop update* [1], in this work we will focus in the first and the last one type of updates.

4.4.1.1 Diagonal updates

The purpose of the diagonal updates is to change the number n of $\hat{\mathcal{O}}_j$ operators in the sequence, where $\hat{\mathcal{O}}_j$ is either $\hat{\mathcal{H}}_{1,b}$, $\hat{\mathcal{H}}_{2,b}$ or the identity $\hat{I}_j$. The simplest way to do this is to substitute unit operators by diagonal operators and vice versa, the insertion of a diagonal operator acting on a bond b requires that the spins at this bond are in an antiparallel state in the propagated state $|\alpha(p)\rangle$ [3]. Graphically this procedure can be seen as follows

Once one has kept track of the propagated states, is natural to carry out the diagonal updates sequentially. Off-diagonal operators cannot be inserted or removed one by one, so they are left unchanged in this update. So, replacing Eqs. (4-14) in Eq. (4-6) we obtain

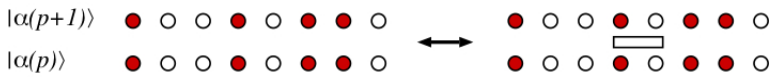

Figure **4-1**: Diagonal update. An operator is either inserted (see from left to right), at a randomly selected bond or removed (see from right to left). If the spins at the chosen bond are parallel the update is cancelled because in one case will leave the spins unchanged, and in the other case will produce a configuration that do not preserves the total spin along $\hat{S}^z$. This figure appears as FIGURE 60 in [1].

$$\mathcal{W}(M, n_1, n_2) = \frac{(-\beta)^2 (M-n)}{M!} \left(-\frac{J}{2}\right)^{n_1} \left(-\frac{J}{2}\right)^{n_2},$$

where $n \equiv n_1 + n_2$. Since both operators have the same weight, the total weight is given by the total number of operators n

$$\mathcal{W}(M, n_1, n_2) = \left(\frac{\beta J}{2}\right)^n \frac{(M-n)!}{M!}. \tag{4-20}$$

The probability of accepting an update using the Metropolis algorithm of Eq. (4-19) is given by

$$\mathcal{A}(x \to x') = \min\left(1, \frac{\mathcal{W}_{new}(x') g_{remove}(x' \to x)}{\mathcal{W}_{current}(x) g_{insert}(x \to x')}\right), \tag{4-21}$$

where $\mathcal{W}_{current}$ and $\mathcal{W}_{new}$ denote the weight of the current and new configuration, respectively, they can be calculated using Eq. (4-20) as follows

$$\mathcal{W}_{current} = \left(\frac{\beta J}{2}\right)^n \frac{(M-n)!}{M!}, \quad \text{and} \quad \mathcal{W}_{new} = \left(\frac{\beta J}{2}\right)^{n+1} \frac{(M-n-1)!}{M!}. \tag{4-22}$$

On the other hand, g_{insert} and g_{remove} represent the probability of insert and remove a diagonal operator, respectively and are given by

$$g_{insert} = \frac{1}{N_b}, \quad \text{and} \quad g_{remove} = 1. \tag{4-23}$$

We choose that value for g_{insert} since there are N_b bonds and we select one at random, and g_{remove} is set to one since we will always attempt to remove a diagonal operator. Then, replacing Eqs. (4-22) and (4-23) in Eq. (4-21) we obtain

$$\mathcal{A}_{insert} = \min\left(1, \frac{\beta J N_b}{2(M-n)}\right) \tag{4-24}$$

On the other hand, if there is already a diagonal operator present, we will attempt to remove it with probability $\mathcal{A}_{remove}$ with the corresponding weights given by

$$\mathcal{W}_{current} = \left(\frac{\beta J}{2}\right)^n \frac{(M-n)!}{M!}, \quad \text{and} \quad \mathcal{W}_{new} = \left(\frac{\beta J}{2}\right)^{n-1} \frac{(M-n+1)!}{M!}, \tag{4-25}$$

and the probabilities

$$g_{insert} = \frac{1}{N_b}, \quad \text{and} \quad g_{remove} = 1. \tag{4-26}$$

The probability of accepting the removal a diagonal operator using the Metropolis algorithm of Eq. (4-19) is given by

$$\mathcal{A}(x \to x') = \min\left(1, \frac{\mathcal{W}_{new}(x') g_{insert}(x \to x')}{\mathcal{W}_{current}(x) g_{remove}(x' \to x)}\right). \tag{4-27}$$

Then, replacing Eqs. (4-25) and (4-26) in Eq. (4-27) we obtain

$$\mathcal{A}_{remove} = \min\left(1, \frac{2(M-n+1)}{\beta J N_b}\right). \tag{4-28}$$

4.4.1.2 Off-diagonal updates: Loop updates

The loop updates change both types of operators, diagonal, and off-diagonal without modify the bonds on which they operate. A major advantage of this kind of update is that changes several operators at the same time. The main idea is to construct a loop connecting vertex legs. Each leg of a vertex is linked to another leg, forming a segment of the loop's path. This procedure can be repeated several times until a closed loop will eventually be formed [28].

As seen in the configuration at the left of figure **4-2**, the spins at all the vertex legs covered by this path (solid red line) can be flipped, which, for operators encountered only once, corresponds to changing the operator type, diagonal to off-diagonal and vice versa. For operators encountered twice (which is the case with the one at $p = 7$), all four spins are flipped, and the operator type then remains unchanged.

It is clear from Fig. **4-2** that each vertex leg uniquely belongs to a single loop. It is thus appropriate to construct all the loops and flip each of the associated spins with probability $1/2$. This is analogous to the Swendsen-Wang cluster update for the classical Ising model [62, 63]. In the classical case, it is often more efficient to use the Wolff algorithm, where clusters are constructed at random (with different randomly chosen starting sites from which the cluster is built up) and flip the associated spins with probability 1 [63, 64].

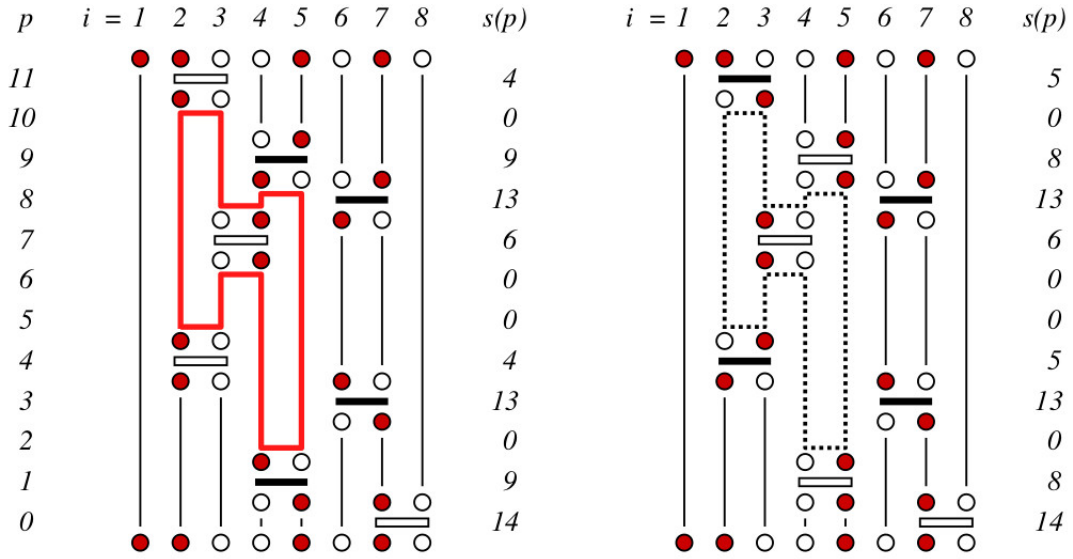

Figure **4-2**: Loop update. All spins covered by the loop are flipped, and operators are changed, diagonal to off-diagonal and vice versa, each time the loop passes by (with no net change of an operator visited twice). Every vertex leg (spin) belongs uniquely to one loop and spins not acted upon by any operator (here the one at i = 1) can also be regarded as forming their own loops. This figure appears as FIGURE 61 in [1].

4.5 SSE for the isotropic spin-1/2 Heisenberg model with external magnetic field

Now, we will extend the SSE QMC method for the (sublattice-rotated) Heisenberg model in the presence of an external magnetic field $\vec{h} = h\hat{z}$. The Hamiltonian can be written as

$$\hat{\mathcal{H}}_{J,h} = -J \sum_{<j,k>} \left[\frac{1}{4} - \hat{S}_j^z \hat{S}_k^z + \frac{1}{2} \left(\hat{S}_j^+ \hat{S}_k^- + \hat{S}_j^- \hat{S}_k^+ \right) \right] - h \sum_j \hat{S}_j^z \tag{4-29}$$

As before, we must write the Hamiltonian in terms of the number of bonds n_b. Therefore, we use $\hat{S}_j^z = (\hat{S}_j^z + \hat{S}_k^z)/2$, replace the sum over nearest neighbors and the sum over lattice sites by a sum over the bonds, b, as follows

$$\hat{\mathcal{H}}_{J,h_b} = \sum_b \left[-J \left(\frac{1}{4} - \hat{S}_{j(b)}^z \hat{S}_{k(b)}^z + \frac{1}{2} \left(\hat{S}_{j(b)}^+ \hat{S}_{k(b)}^- + \hat{S}_{j(b)}^- \hat{S}_{k(b)}^+ \right) \right) - h_b \left(\hat{S}_{j(b)}^z + \hat{S}_{k(b)}^z \right) \right], \tag{4-30}$$

where we have defined $h_b \equiv h/2b$ to avoid double counting (since each spin now appears in $2b$ bonds). Now we can write $\mathcal{H}$ as the sum of diagonal and off-diagonal components

$$\hat{\mathcal{H}}_{J,h_b} = \sum_b (\hat{\mathcal{H}}_{1,b} + \hat{\mathcal{H}}_{2,b}), \tag{4-31}$$

with

$$\hat{\mathcal{H}}_{1,b} = -J\left(\frac{1}{4} - \hat{S}^z_{j(b)}\hat{S}^z_{k(b)}\right) - h_b\left(\hat{S}^z_{j(b)} + \hat{S}^z_{k(b)}\right), \tag{4-32}$$

and

$$\hat{\mathcal{H}}_{2,b} = -\frac{J}{2}\left(\hat{S}^+_{j(b)}\hat{S}^-_{k(b)} + \hat{S}^-_{j(b)}\hat{S}^+_{k(b)}\right). \tag{4-33}$$

To ensure that all non-zero matrix elements will be negative, we must subtract a constant $-\mathcal{C}$ to the diagonal term

$$\hat{\mathcal{H}}_{J,h_b,\mathcal{C}} = -\mathcal{C}n_b + \sum_b \left(\hat{\mathcal{H}}_{1,b} + \hat{\mathcal{H}}_{2,b}\right) \equiv \hat{\mathcal{H}}. \tag{4-34}$$

When taking measurements, in order to get the correct energy value it is necessary to add an offset of $n_b\,\mathcal{C}$ to the measured value of the energy. The vertex corresponding to the diagonal terms can be written as

$$\left\langle ++\left|\hat{\mathcal{H}}\right|++\right\rangle = -\mathcal{C} - h_b, \quad \text{and} \quad \left\langle --\left|\hat{\mathcal{H}}\right|--\right\rangle = -\mathcal{C} + h_b, \tag{4-35}$$

and the vertex corresponding to the non-diagonal terms satisfy

$$\left\langle \pm\mp\left|\hat{\mathcal{H}}\right|\pm\mp\right\rangle = -\mathcal{C} - \frac{J}{2}, \quad \text{and} \quad \left\langle \pm\mp\left|\hat{\mathcal{H}}\right|\mp\pm\right\rangle = -\frac{J}{2}. \tag{4-36}$$

From now on we set $h_b \geq 0$, then, from Eqs. (4-35) and (4-36) we see that to guarantee that all these vertices are negative $\mathcal{C} \geq h_b$. It is convenient to define $\mathcal{C} = \mathcal{C}_0 + \epsilon$ with $\mathcal{C}_0 = h_b$ and the constant ϵ represents the excess over the minimum value $\mathcal{C}_0$. In this way, the vertex given in Eqs. (4-35) and (4-36) takes the form

$$\left\langle ++\left|\hat{\mathcal{H}}\right|++\right\rangle = -\epsilon \quad \text{and} \quad \left\langle --\left|\hat{\mathcal{H}}\right|--\right\rangle = -\epsilon - 2h_b, \tag{4-37}$$

and

$$\left\langle \pm\mp\left|\hat{\mathcal{H}}\right|\mp\pm\right\rangle = -\frac{J}{2} \quad \text{and} \quad \left\langle \pm\mp\left|\hat{\mathcal{H}}\right|\pm\mp\right\rangle = -\frac{J}{2} - h_b - \epsilon, \tag{4-38}$$

respectively.

4.5.1 Diagonal updates

The diagonal update procedure is like the one discussed in previous section for pure Heisenberg model (without external magnetic field) with a few key differences. We can calculate the weight of a given configuration as a function of the number of operators of each type that it contains, using Eqs. (4-38) we obtain

$$\begin{aligned}\mathcal{W}(n_1,n_2,n_3,n_4) &= \frac{(-\beta)^n(M-n)!}{M!}(-\epsilon)^{n_1}(-\epsilon-2h_b)^{n_2}\left(-\epsilon-\frac{J}{2}-h_b\right)^{n_3}\left(-\frac{J}{2}\right)^{n_4} \\ &= \frac{\beta^n(M-n)!}{M!}(\epsilon)^{n_1}(\epsilon+2h_b)^{n_2}\left(\epsilon+\frac{J}{2}+h_b\right)^{n_3}\left(\frac{J}{2}\right)^{n_4}, \end{aligned} \tag{4-39}$$

where $n = n_1 + n_2 + n_3 + n_4$. The minus signs from the individual operator weights and the present in the pre-factor $(-\beta)^n$ compensate each other. Unlike in the pure Heisenberg model, there are now six different types of diagonal operators. At each time slice if no operator is present, we select a bond at random and attempt to insert the appropriate type of operator with a probability that obeys the detailed balance condition. We use the following indexation, see Table **4-1**, in order to identify each vertex. Note that the operators of type 1, 2, 3 and 6, correspond to diagonal operators, while 4 and 5 are off-diagonal operators. As before, the insertion probabilities can be calculated using Eq. (4-21). After some algebra we obtain the following insertion probabilities for the diagonal operators

Type	Vertice	Value
1	$\langle\downarrow\downarrow\|\hat{\mathcal{H}}\|\downarrow\downarrow\rangle$	$-\epsilon-2h_b$
2	$\langle\downarrow\uparrow\|\hat{\mathcal{H}}\|\downarrow\uparrow\rangle$	$-J/2-h_b-\epsilon$
3	$\langle\uparrow\downarrow\|\hat{\mathcal{H}}\|\uparrow\downarrow\rangle$	$-J/2-h_b-\epsilon$
4	$\langle\downarrow\uparrow\|\hat{\mathcal{H}}\|\uparrow\downarrow\rangle$	$-J/2$
5	$\langle\uparrow\downarrow\|\hat{\mathcal{H}}\|\downarrow\uparrow\rangle$	$-J/2$
6	$\langle\uparrow\uparrow\|\hat{\mathcal{H}}\|\uparrow\uparrow\rangle$	$-\epsilon$

Table **4-1**: Vertices of the SSE for the isotropic spin-1/2 Heisenberg model with external magnetic field. The operators of type 1, 2, 3 and 6 correspond to diagonal operators and the type 4 and 5 to off-diagonal ones.

$$\mathcal{A}^{(6)}_{insert} = \min\left(1, \frac{2n_b\beta\epsilon}{M-n}\right) \tag{4-40}$$

$$\mathcal{A}^{(1)}_{insert} = \min\left(1, \frac{2n_b\beta}{M-n}(\epsilon+2h_b)\right) \tag{4-41}$$

$$\mathcal{A}^{(2,3)}_{insert} = \min\left(1, \frac{2n_b\beta}{M-n}\left(\epsilon+\frac{J}{2}+h_b\right)\right). \tag{4-42}$$

The probabilities associated to the removal of diagonal operators are given by Eq. (4-27). We found

$$\mathcal{A}^{(6)}_{remove} = \min\left(1, \frac{M-n+1}{2n_b\beta\epsilon}\right) \tag{4-43}$$

$$\mathcal{A}^{(1)}_{remove} = \min\left(1, \frac{M-n+1}{2n_b\beta}\left(\epsilon + 2h_b\right)\right) \tag{4-44}$$

$$\mathcal{A}^{(2,3)}_{remove} = \min\left(1, \frac{M-n+1}{2n_b\beta}\frac{1}{\left(\epsilon + \frac{J}{2} + h_b\right)}\right). \tag{4-45}$$

The updating scheme is like that for the pure Heisenberg model with a few differences. For example, in the diagonal updates of the pure Heisenberg model there was only two types of diagonal operators, corresponding to anti-parallel spins (type 2 and 3 vertex). However, for non-zero field we have six different vertices. Therefore, the updating scheme for non-zero magnetic field requires to verify the vertex type.

The type 4 and 5 vertices correspond to off-diagonal operators, in this case the probability does not change at all, is the same showed before in Eq. (4-24), then

$$\mathcal{A}^{(4,5)}_{insert} = \min\left(1, \frac{\beta J N_b}{2(M-n)}\right) \quad \text{and} \quad \mathcal{A}^{(4,5)}_{remove} = \min\left(1, \frac{2(M-n+1)}{\beta J N_b}\right). \tag{4-46}$$

4.5.2 Off-diagonal updates

For the off-diagonal updates it is necessary an entirely new procedure. In the pure Heisenberg model, we could build loops and flip the associated spins with probability 1/2 because diagonal and off-diagonal operators had the same weight, see Eqs. (4-14). Consequently, change any number of diagonal operators to off-diagonal operators, and vice versa, does not alter the weight of the configuration, Eq. (4-20). For the case of non-zero external magnetic field, this is no longer true. We can still construct the loops as we did before and decide how to flip them using the Metropolis condition. An issue that arises from this approach is that loops change many operators and, therefore, change the energy by a large amount causing the loop acceptance probability to become quite small [58].

In the loop updates for pure Heisenberg model, the loops are constructed deterministically but they are flipped stochastically. In contrast, for the Heisenberg model with magnetic field, the loops are constructed stochastically. When a loop is closed, detailed balance condition is already satisfied and the loops can be flipped with probability 1 [2]. A major advantage of this procedure is that no time is wasted constructing loops that are never flipped.

4.5.2.1 Constructing the loops stochastically

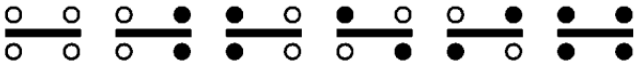

Figure **4-3**: The six different vertices corresponding to the matrix elements in Eqs. (4-38). The horizontal bar represents the operator acting in the bond and the circles represent the spin state, solid and open circles for spin-up and spin-down, respectively. This figure appears as FIG 1. in [2].

The basic idea of the off-diagonal operators update scheme works as follows. You start by choosing a vertex leg at random, “entrance” leg, and flip it. For example, let us say you start (enter) on the lower left leg of a vertex, see Figure **4-3**, the resulting vertex is invalid, since do not conserves the total spin. To correct this, we must choose a second leg to flip, the “exit” leg. There are four ways choose this leg:

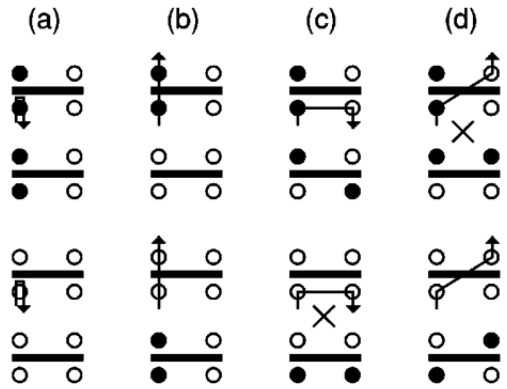

Figure **4-4**: All four paths through two vertices where the entrance is at the lower left leg. The arrow indicates the exit leg. The resulting updated vertices, with the spin at the entrance and exit legs flipped, are also shown. The two cases marked with an X are forbidden, since the updated vertices do not conserve the total spin along $\hat{S}^z$. This figure appears as FIG 3. in [2].

We could

- *Bounce*: exiting on the leg we came in on, producing the same vertex with which we started.
- *Continue straight*: exiting on the opposite leg of the “entrance leg”.
- *Switch and reverse*: exiting on the side neighbour of the “entrance” leg.
- *Switch and continue*: exiting on the opposite by the diagonal leg of the “entrance” leg.

After this, we follow the exit leg until reach a new entrance leg, selecting the respective exit leg and repeating this process until we return to the leg we started on. It may happen that a given vertex is visited more than once. This procedure have the advantage that we will not construct loop that will not be flipped, like in the pure Heisengber model. Depending on the type of vertex we are the probabilities of Eqs. (4-41), (4-42), (4-46) and (4-40) will represent one of the four processes mentioned before. In the Appendix C we show the probabilities associated to the four processes for each type of vertex.

4.6 Code implementation

In this section we comment the most important details to consider in the code implementation of the SSE QMC algorithm. In this project we use as starting point a Fortran code provided by the author of the SSE method, Anders W. Sandvik, that can be found in his website [65]. The Sandvik’s code provides an SSE QMC implementation for the spin-1/2 Heisenberg model, we modified it in order to include the presence of a magnetic field.

The computational expense of SSE is polynomial in system size L and inverse temperature $\beta = 1/T$, scaling as βL^d [58]. SSE also can be used to access zero-temperature properties by exploiting the

gap between the ground state and the first excited state that appears in finite-size systems. Typically $\Delta \propto 1/L$, so zero-temperature properties appears when $T \ll \Delta$ i.e. $\beta \gg L$ at a computational cost that scales $\tau \propto L^{d+1}$ [58].

4.6.1 Main program

In the figure **4-5** we present the scheme of the main function of the SSE QMC method for the isotropic spin-1/2 Heisenberg model with a magnetic field. The SSE QMC algorithm can be divided into three parts: Module configuration, equilibration phase, and measurement phase. In the next section we will briefly explain each of them.

4.6.2 Module configuration

In the module configuration we define all the parameters and data structures, such as the lattice dimensions N, the system temperature T, the magnitude of the magnetic field h_b, etc.

In the SSE program, the operator products in the partition function $\prod_{p=1}^{M} \hat{\mathcal{H}}_{a(p),b(p)}$ are represented by a one-dimensional integer array opstring[p] [3], with $p = 1, 2, 3, ..., M$, where both indices a and b are encoded into a single integer according to

$$\text{opstring[p]} = 2\text{b(p)} + \text{a(p)} - 1.$$

In this way, even and odd valued elements correspond to diagonal and off-diagonal operators, respectively. The identity operator $(a = b = 0)$ is encoded as opstring[p]=0. The spin state $|\alpha\rangle$ of the system is represented by the array spin[i], $i = 1, ..., N$, with elements $+1$ and -1 corresponding to spin up and down

$$\text{spin[i]} = 2\hat{S}_j^z.$$

The representation of the current SSE configuration by the arrays spin[] and opstring[] is used throughout the program. From these, any propagated state can be generated as needed.

4.6.2.1 Equilibration phase

In the equilibration phase we sweep up the system from its initial state (AFM vacuum) until it reaches the equilibrium state. To do that, in each iteration (timeslice) we begin applying the diagonal update to insert/remove diagonal operators, then, we proceed construct the vertex linked-list in order to determine how the operators are connected, see Appendix D. Knowing how the vertices are connected, we proceed to perform the loop update and finally adjust the cutoff of the expansion.

It is necessary to clarify what we mean by “adjust the cutoff of the expansion”. Note that to make inserting and removing operators easier, we must fix M. M is the number of complete set of states (“cutoff”). The cutoff M must be larger than the largest order of the expansion (n), so this procedure is exact and does not introduce any error.

In practice, M can be determined automatically during the equilibration phase of the simulation by setting

$$M = \frac{4}{3} n_{max}, \tag{4-47}$$

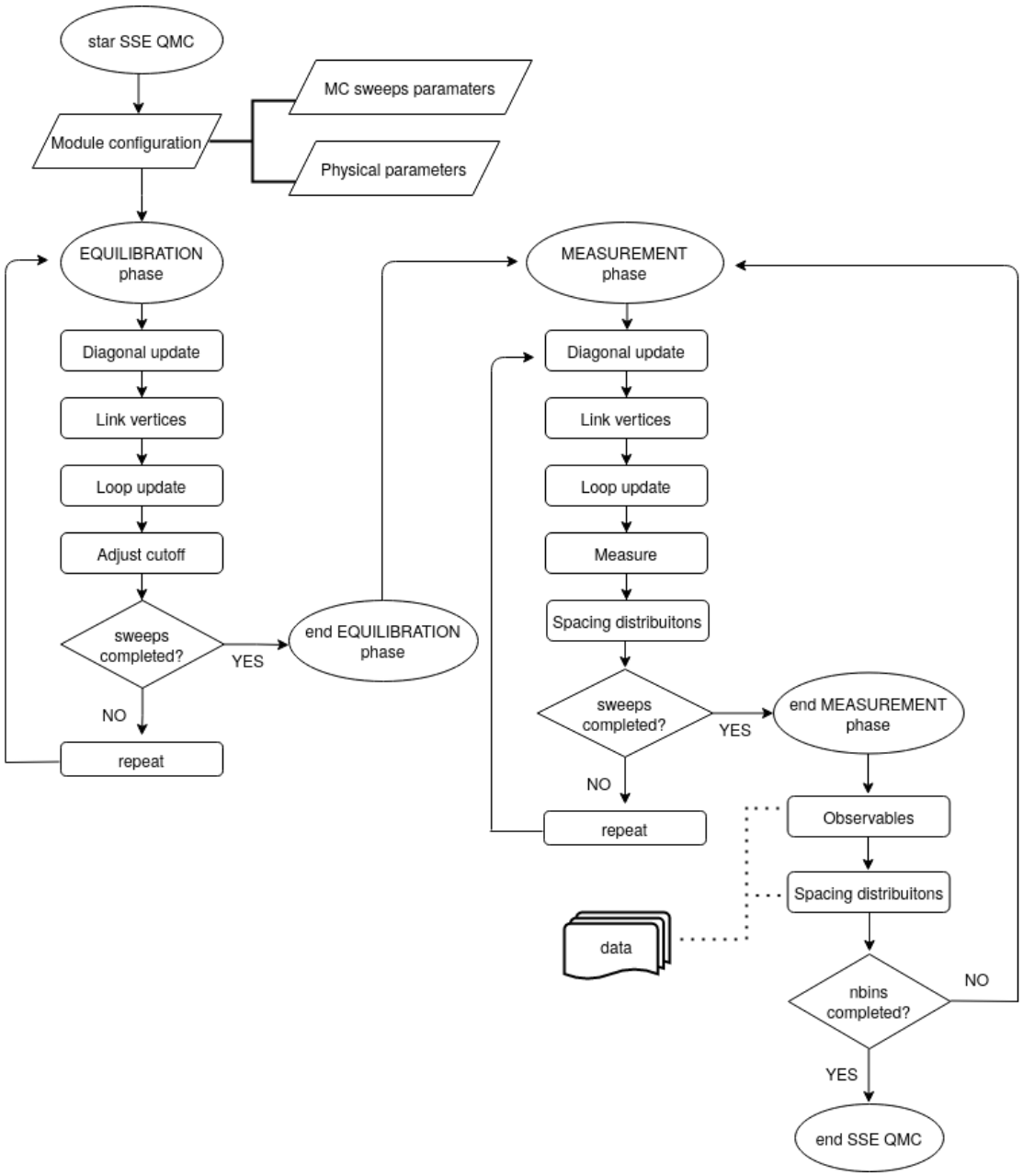

Figure **4-5**: Main program of the SSE QMC method for the isotropic spin-1/2 Heisenberg model with an external magnetic field.

where n_{max} is the largest value of n reached [58]. After the equilibration phase, the cutoff must be fixed to avoid biasing the simulation, in ref. [3] is shown that the cutoff can be adjusted as follows

$$M_{new} = nh + \frac{nh}{3}, \tag{4-48}$$

where nh denotes the number of diagonal operators in the simulation. Once the isteps iterations are completed, we move to the measurement phase.

4.6.2.2 Measurement phase

The measurement phase is quite similar to the equilibrium phase since we perform again the corresponding diagonal updates, generate the vertex linked list and construct the loops for the loop update. However, in this phase we have not to adjust the cutoff anymore since we already have reached the equilibrium. Then, we finalize this phase measuring the observables and the spacing distributions. The information provided by the simulation will be storage in "bins" and then calculate the mean values as the average of bins. The bins must be understood as the number of times that we perform measures in the same system.

4.7 Observables in the SSE QMC algorithm

Consider the expectation value of an arbitrary function f

$$\langle f \rangle = \frac{1}{\mathcal{Z}_N(\beta)} \sum_{\{\sigma\}} f(\sigma) e^{-\beta E(\sigma)}, \tag{4-49}$$

where $\mathcal{Z}_N(\beta)$ is the partition function, as defined before, and σ includes all the degrees of freedom of the system, $E(\sigma)$ is the energy, and $\beta = 1/T$ is the inverse temperature (using dimensionless units). We can evaluate the expectation value of Eq. (4-49) using the Metropolis algorithm, according to the Boltzmann probability distribution given by

$$P(\sigma) = \frac{1}{\mathcal{Z}_N(\beta)} \mathcal{W}(\sigma), \quad \text{with} \quad \mathcal{W}(\sigma) = e^{\beta E(\sigma)}. \tag{4-50}$$

The expectation value is then simply obtained as the average of the function $f(\sigma)$ over the sampled configurations $\sigma(j)$, $i = 1, ..., N$. Therefore

$$\langle f \rangle = \frac{1}{N} \sum_{j} f(\sigma(j)). \tag{4-51}$$

In most of the cases, we are not able to evaluate the exponential function. If we can evaluate any power of a number, we could Taylor expand the exponential and write the expectation value as

$$\langle f \rangle = \frac{1}{\mathcal{Z}_N(\beta)} \sum_{\{\sigma\}} \sum_{N=0}^{\infty} f(\sigma) \frac{(-\beta E)^n}{n!}, \quad \text{with} \quad \mathcal{Z}_N(\beta) = \sum_{\{\sigma\}} \sum_{N=0}^{\infty} \frac{(-\beta E)^n}{n!}. \tag{4-52}$$

We can think of this as having enlarged our configuration space into an “expansion dimension” where the coordinate to be sampled is the power n [3]. We can thus carry out a Monte Carlo sampling in the configuration space (σ, n).

This approach work provided that all the terms in the sum are positive, which requires the energy to always be negative. This is not always satisfied. However, we can always subtract a constant ϵ from the energy without changing the physics of the system. Choosing the constant $\epsilon > 0$ properly, the weight used for sampling the extended configuration space is

$$\mathcal{W}(\sigma, n) = \frac{\beta^n(\epsilon - E(\sigma))^n}{n!}. \tag{4-53}$$

4.7.1 Non-diagonal observables

Non-diagonal observables do not have an obvious classical analogue. Constructing estimators for off-diagonal observables is therefore somewhat tricky. In many cases, diagonal observables suffice or there are easier to measure substitutes for an off-diagonal observable [58]. For example, in the isotropic zero-field Heisenberg model, there is full $\mathcal{O}(3)$ rotational symmetry, therefore $\left\langle \left| \vec{S} \right| \right\rangle = 3 \left\langle \left| \vec{S}_z \right|^2 \right\rangle$ without directly calculate the $\hat{x}$ and $\hat{y}$ components. Alternatively, in the Heisenberg model with an external magnetic field, we cannot rely on symmetry to extract the spin correlation length in the XY plane.

However, non-diagonal observables that appear as terms in the Hamiltonian, can often be measured in a simple way. The best example is the energy, which is obviously not diagonal in the $\hat{S}_z$ basis.

4.7.1.1 Average Energy

The expectation value of the energy is given by

$$E = \left\langle \hat{\mathcal{H}} \right\rangle = \frac{1}{\mathcal{Z}_n(\sigma)} \sum_{\sigma,n} \hat{\mathcal{H}}(\sigma)\mathcal{W}(\sigma, n), \tag{4-54}$$

where

$$\mathcal{Z}_n(\sigma) = \sum_{\sigma,n} \mathcal{W}(\sigma, n), \quad \text{and} \quad \mathcal{W}(\sigma, n) = \frac{\beta^n \hat{\mathcal{H}^n}(\sigma)}{n!}. \tag{4-55}$$

By shifting the summation index to $m = n + 1$, we obtain

$$\sum_{\sigma,n} \hat{\mathcal{H}}(\sigma)\mathcal{W}(\sigma, n) = \sum_{\sigma,m} \frac{m}{\beta} \mathcal{W}(\sigma, m). \tag{4-56}$$

Thus, the Eq. (4-56) transforms as follows

$$\left\langle \hat{\mathcal{H}} \right\rangle = \frac{1}{\beta} \langle n \rangle_{\mathcal{W}}. \tag{4-57}$$

Finally, using Eq. (4-55) in Eq. (4-56) we obtain

$$E = \epsilon - \frac{1}{\beta}\langle n\rangle_{\mathcal{W}}\,, \quad \text{with} \quad \langle n\rangle_{\mathcal{W}} = \frac{m\beta}{\mathcal{Z}_n(\sigma)}\mathcal{W}(\sigma, m), \tag{4-58}$$

where ϵ is a shift in the energy that do not alters the spectrum and can be removed conveniently when measurements are taken. We conclude that, if $f(\sigma)$ is a function of the energy, one can rewrite the expectation value as function that depends only n.

4.7.1.2 Heat capacity

Finally, lets calculate an expression for the expectation value of $\hat{\mathcal{H}}^2$.

$$\left\langle \hat{\mathcal{H}}^2 \right\rangle = \frac{1}{\mathcal{Z}_N(\beta)}\sum_{n,\sigma}\hat{\mathcal{H}}^2(\sigma)\mathcal{W}^2(\sigma, n), \tag{4-59}$$

the term of the sum can be written as follows

$$\begin{aligned}\hat{\mathcal{H}}(\sigma)\mathcal{W}(\sigma, n) &= \hat{\mathcal{H}}(\sigma)\frac{\beta^{m-1}\mathcal{H}^{m-1}(\sigma)}{(m-1)!} \\ &= \frac{1}{\beta}\frac{m!}{(m-1)!}\frac{\beta^m\mathcal{H}^m(\sigma)}{m!} \\ &= \frac{m}{\beta}\mathcal{W}(\sigma, m)\end{aligned} \tag{4-60}$$

Proceeding as above, we write the sum of Eq. (4-59) in terms of a shifted summation index $m = n + 2$ and replacing Eq. (4-60) we obtain

$$\left\langle \hat{\mathcal{H}}^2 \right\rangle = \frac{1}{\beta^2}\langle n(n+1)\rangle_{\mathcal{W}}\,. \tag{4-61}$$

As usual, the heat capacity is given by

$$\mathcal{C} = \beta^2\left(\left\langle \hat{\mathcal{H}}^2 \right\rangle - \left\langle \hat{\mathcal{H}} \right\rangle^2\right), \tag{4-62}$$

replacing Eqs. (4-57) and (4-61) in Eq. (4-62) we obtain

$$\mathcal{C} = \langle n^2\rangle - \langle n\rangle^2 - \langle n\rangle\,. \tag{4-63}$$

4.8 Spacing-distributions in the SSE QMC algorithm

In the initial state corresponds to an antiferromagnetic state, i.e., a pattern of alternating up-down spins. Then, the algorithm described previously evolves the system until reaches the equilibrium. The spacing distributions can be measured directly from the spin configurations. We measure the domain size distribution for spins up

$$p_n^0 = \mathcal{P}(\downarrow \overbrace{\uparrow \cdots \uparrow}^{n} \downarrow), \tag{4-64}$$

and for spins down

$$p_n^0 = \mathcal{P}(\uparrow \overbrace{\downarrow \cdots \downarrow}^{n} \uparrow). \tag{4-65}$$

As mentioned before, an interesting regime appears as $2\,h$ gets close to J from below, consecutive domains of spins parallel to the field are separated each other by a single spin pointing in the opposite direction. In this analogy the minority spins are represented by particles, while the spins parallel to the field by empty sites. Therefore, we can define another quantity that also provides information about the structure formed by the domains, the probability p_n^1. By definition p_n^1 is the probability to find two consecutive domains separated by a single spin in opposite direction with a total length n.

$$p_n^1 = \sum_m \mathcal{P}(\downarrow \overbrace{\uparrow \cdots \uparrow}^{m-1} \downarrow \overbrace{\uparrow \cdots \uparrow}^{n-m+1} \downarrow). \tag{4-66}$$

Another distribution that can be used to describe the system is the probability of two consecutive domains with a total length n

$$Q(L) = \sum_{l=1}^{L} \mathcal{P}(\downarrow \overbrace{\uparrow \cdots \uparrow}^{l} \overbrace{\downarrow \cdots \downarrow}^{L-l} \uparrow). \tag{4-67}$$

Unfortunately, $Q(L)$ cannot be evaluated as easily as the distributions p_n^0 and p_n^1 except for the trivial high temperature regime.

Chapter 5

Results

In this chapter we present the results of the computational simulation given by the implementation of the SSE QMC algorithm for the isotropic spin-1/2 Heisenberg model with a magnetic field. We use the thermodynamic observables showed in chapter 1 in order to verify that the algorithm works well, and then, we proceed to present the results obtained for the spacing-distributions presented in Chapter 3.

5.1 Thermodynamic observables

In the simulation 80000 MCS were used to reach the equilibrium, we use $N = 512$, $k_B = 1$ and $J = 1$. Continuous lines correspond to the analytical expression presented in Chapter 1 while dots to the numerical results obtained from the SSE QMC simulation.

As shown in Fig. **5-1**, despite having done the simulation with a small system and few iterations, the results adjust to the theoretical curves obtained in Chapter 1 really nice. For $T = 0$, the internal energy coincides with the ground state energy E_g and, as T increases $\mathcal{U}$ approaches to zero, see Fig. **5-1**. In the limit of high temperatures β is an small parameter and the internal energy reduces to $\mathcal{U} \approx -\beta(h^2 + J^2/8)$. As expected, for $h = 0$ the magnetization is zero for any value of T. For $T = 0$ and $h > 0.5$ the magnetization is equal to one because all the spins are parallel to the field. For $T = 0$ and $0 < h < 0.5$ the magnetization is smaller than one due to the existence of spins down. Naturally, for $T > 0$, the magnetization decreases in comparison with the $T = 0$ case due to the thermal fluctuations which randomize the system, see Fig. **5-1**. In fact, from Eq. (1-38) it is easy to see that for large T, $\mathcal{M} \approx h\beta$. For $h = 0$, $\mathcal{M} = 0$ regardless the value of T because $\rho = 1/2$ and the number of spins up and down are equal. At $T = 0$ we can expect an interesting behavior as $2h$ gets close to J from below. Note that in this regime small changes in h lead to large changes in $\mathcal{M}$. In fact, as seen in Fig. **5-1**, for $h = 0$ the susceptibility diverges at $T = 0$. This fact suggests the existence of critical behavior which is associated to the crossover between the organized state $\mathcal{M} = 1$ $(2h > J)$ and the disorganized state $\mathcal{M} < 1$ $(2h < J)$.

5.2 Spacing-distributions

In the simulation 500000 MCS were used to reach equilibrium, we use $k_B = 1$ and $J = 1$. Continuous lines correspond to the analytical expression obtained by the IPDF method while dots to the numerical

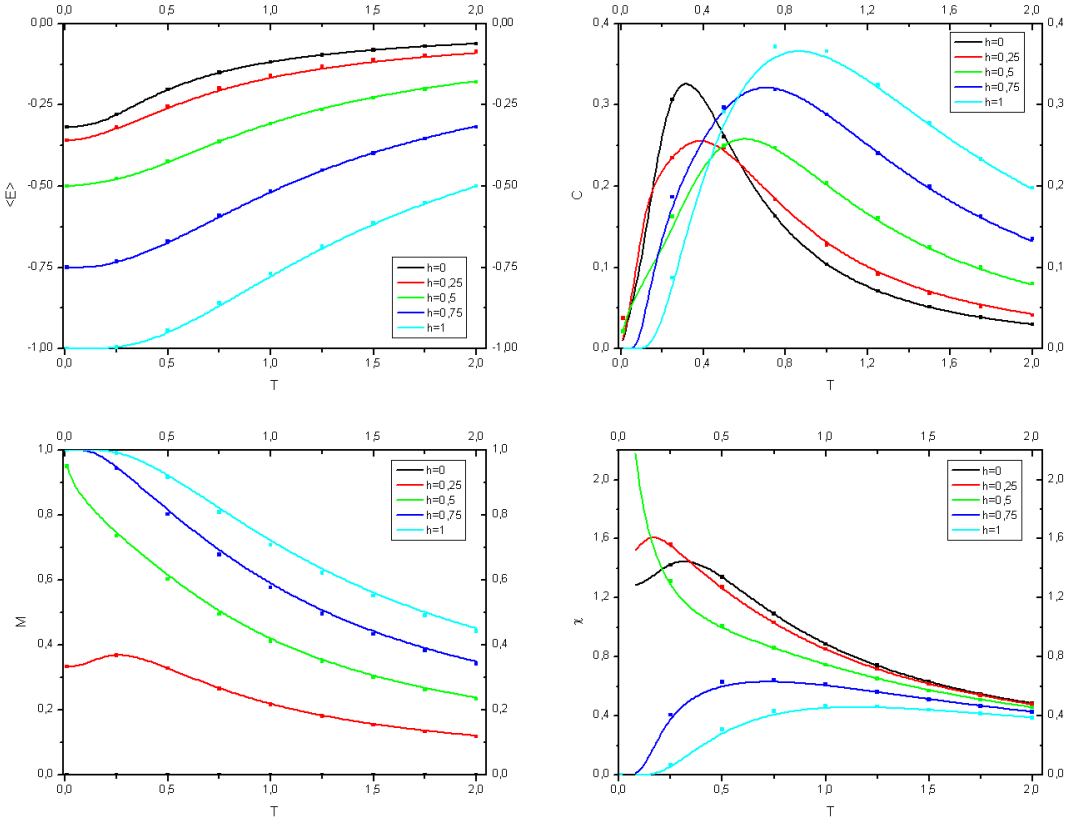

Figure **5-1**: Thermodynamic observables. In the first row from left to right average energy and heat capacity; in the second row, magnetization and magnetic susceptibility.

results obtained from the SSE QMC simulation and the dotted red curves correspond to the GWS.

We perform the simulation for different lattice sizes $N = 64, 128, 512$, then, we set up the magnetic field to $h_b = 0.48$ and the excess over the minimum to $\epsilon = 0.01$ (this value is recommended by Sandvik for this system [2]). We will work in the range of temperatures to $T = 0.01$ (Figures **5-4**,**5-8**,**5-12**), $T = 0.0075$ (Figures **5-5**, **5-9**, **5-13**), $T = 0.005$ (Figures **5-6**, **5-10**, **5-14**) and $T = 0.0025$ (Figures **5-7**, **5-11**, **5-15**).

At high temperatures, it is reasonable to expect that the spins behavior is dominated by the thermal fluctuations. In this regime it is possible to neglect the correlations between adjacent sites. Thus, Eq. (3-9) can be written as

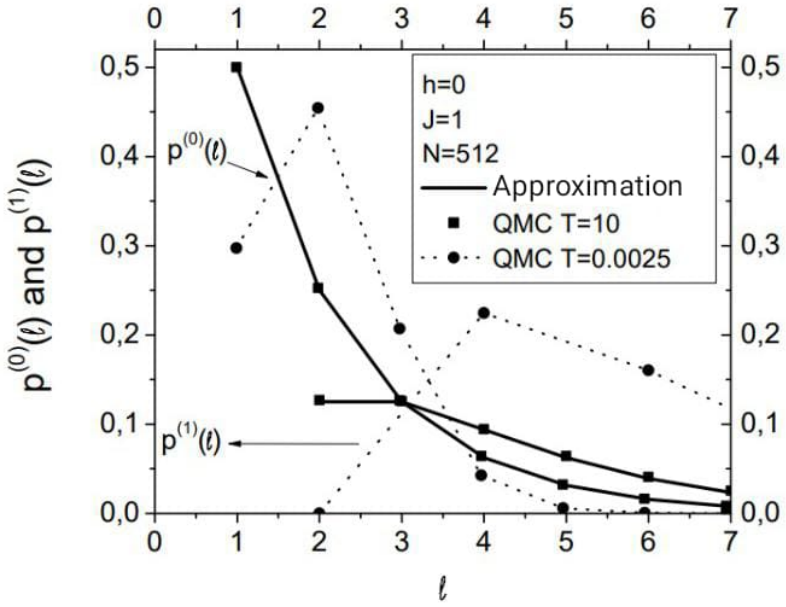

Figure **5-2**: Normalized spacing distributions for $T = 0.0025$ and $T = 10$ with $h = 0$.

$$\begin{aligned} p_n^0 &\approx \left\langle \hat{c}_0^\dagger \hat{c}_0 \right\rangle \prod_{j=1}^{n-1} \left\langle \hat{b}_j^\dagger \hat{b}_j \right\rangle \left\langle \hat{c}_L^\dagger \hat{c}_L \right\rangle \\ &= \rho^2 (1-\rho)^{n-1}. \end{aligned} \tag{5-1}$$

Similarly, the probability Q_n can be approximated as follows

$$\begin{aligned} Q_n &\approx \rho \sum_{l=1}^{n-1} \rho^{n-l} (1-\rho)^l (1-\rho) \\ &= \frac{(\rho-1)\rho\left((1-\rho)^n \rho + \rho^n (\rho-1)^n\right)}{2\rho - 1}. \end{aligned} \tag{5-2}$$

As seen in Fig. **5-2**, Eqs. (5-1) and (5-2) reproduces p_n^0 and Q_n with $h = 0$ and $T = 10$. However, for low temperatures, quantum fluctuations are relevant, and the spacing distributions cannot be approximated by Eqs. (5-1) and (5-2), see dot-lines in Fig. **5-2**. In fact, for high temperatures the spacing distributions decays monotonically which does not occur for small temperatures, indicating that consecutive domains are correlated. At $T = 10$ the most probable length of a domain is one, while for $T = 0.0025$ is two. Clearly, for large T the correlations between adjacent sites can be neglected and the spacing distributions can be calculated easily. In fact, the probability to find two or more consecutive domains can be obtained by using the independent interval approximation where the required distribution is written in terms of the convolution of single domain distributions.

However, the most interesting behavior is found for values of h smaller but close to $J/2$. In this region, the number of fermions is near to zero, i.e., there are domain formation of spins parallel to h. The domain

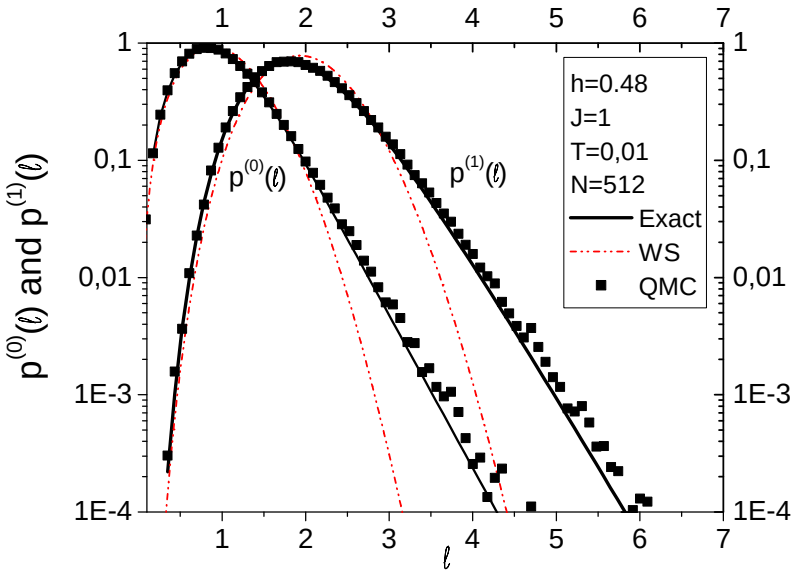

Figure **5-3**: Normalized p_n^0 and p_n^1 spacing-distributions for a chain of size N=512, h=0.48 and T=0.01. The exponential tail appears even for small temperatures and widely deviates from the Gaussian tail of the GWS.

length distribution is given by the inter-particle distribution p_n^0. The probability to find two consecutive domains of spins up separated by a single spin down is given by p_n^1. In the following figures, the continuous lines corresponds to the analytical expression given by Eqs. (3-9) and (3-11) and dots to the QMC simulations. Given the complexity of the analytical expressions for the spacing distributions it is convenient to use the approximate expressions provided by the GWS. The results given by the GWS are include in the figures (dash-dotted red line) to illustrate the quality of the approximation. The logarithmic scale used to highlights the behavior of the distribution for small and large values of n. Note the excellent agreement between the QMC results and the ones given by Eqs. (3-9), (3-11) and the GWS. The logarithmic scale is used to highlight the behavior of the distribution for small and large values of n. At $T = 0$ the spacing distributions have Gaussian right tails but for $T > 0$ they decay exponentially, see Fig. **5-3**. The left tail of the distributions is not affected by the thermal fluctuations, i.e., it has the form $p_n^0 \sim n^2$ and $p_n^1 \sim n^7$ regardless the value of T. Our results suggest that the behavior of effective interaction between spins for large distance strongly depends on temperature while the one for short distances is temperature independent.

As T increases, the thermal fluctuations randomize the system and the right tail of the distribution becomes exponential rather than Gaussian, see the figure **5-3**. However, the behavior for small values remains unchanged.

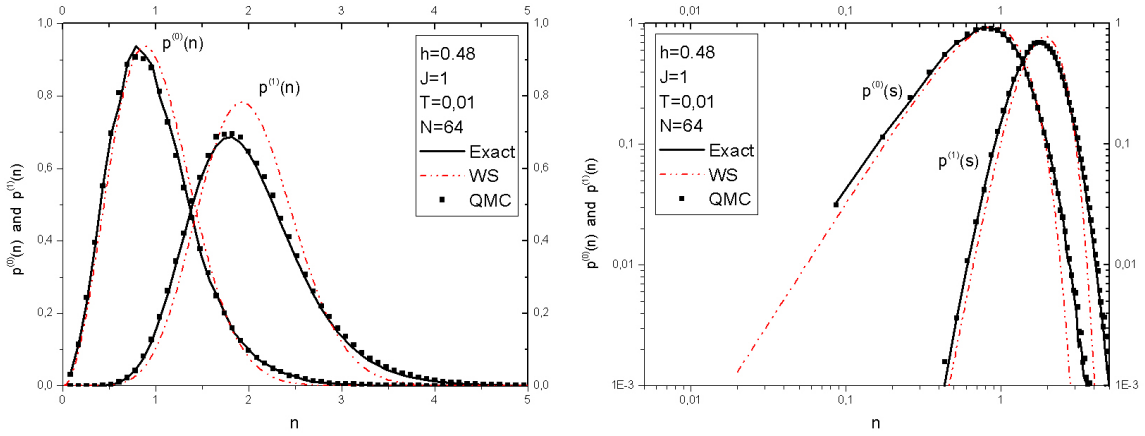

Figure **5-4**: Normalized p_n^0 and p_n^1 spacing-distributions for a chain of size N=64, h=0.48 and T=0.01.

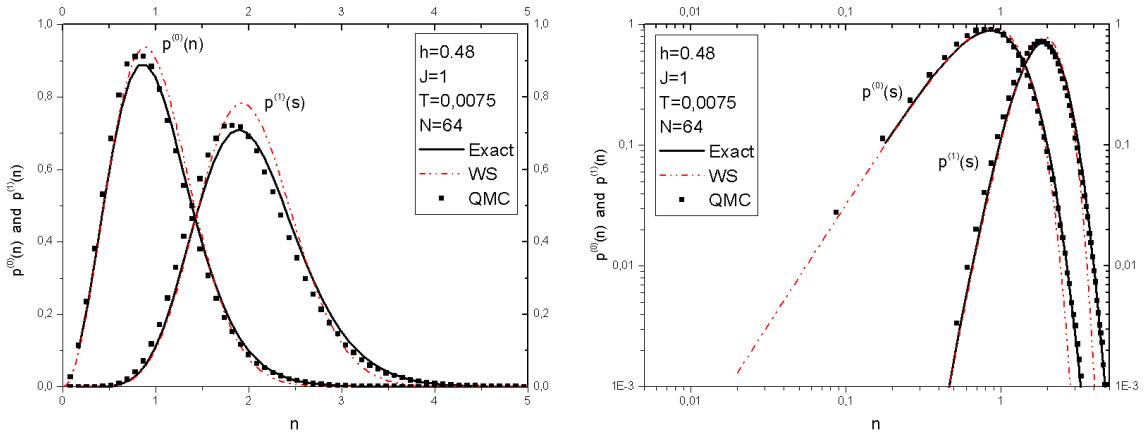

Figure **5-5**: Normalized p_n^0 and p_n^1 spacing-distributions for a chain of size N=64, h=0.48 and T=0.0075.

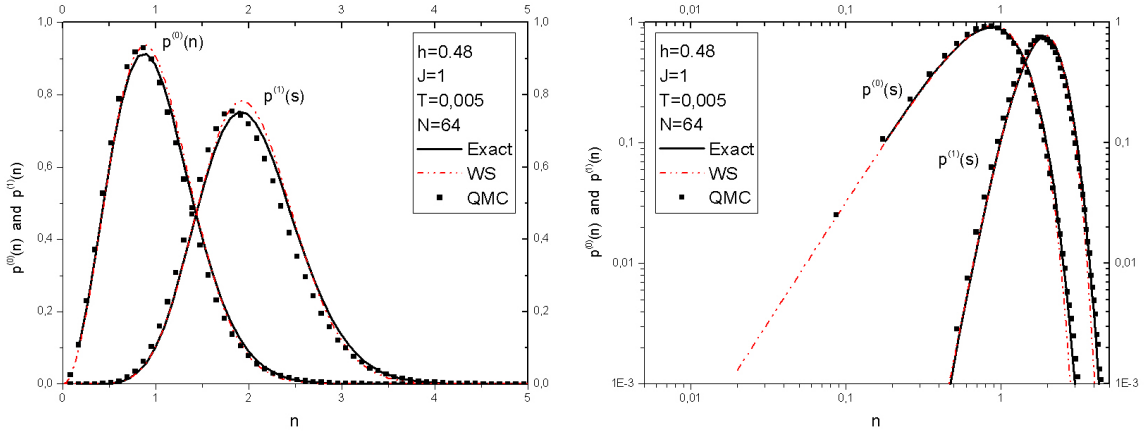

Figure **5-6**: Normalized p_n^0 and p_n^1 spacing-distributions for a chain of size N=64, h=0.48 and T=0.005.

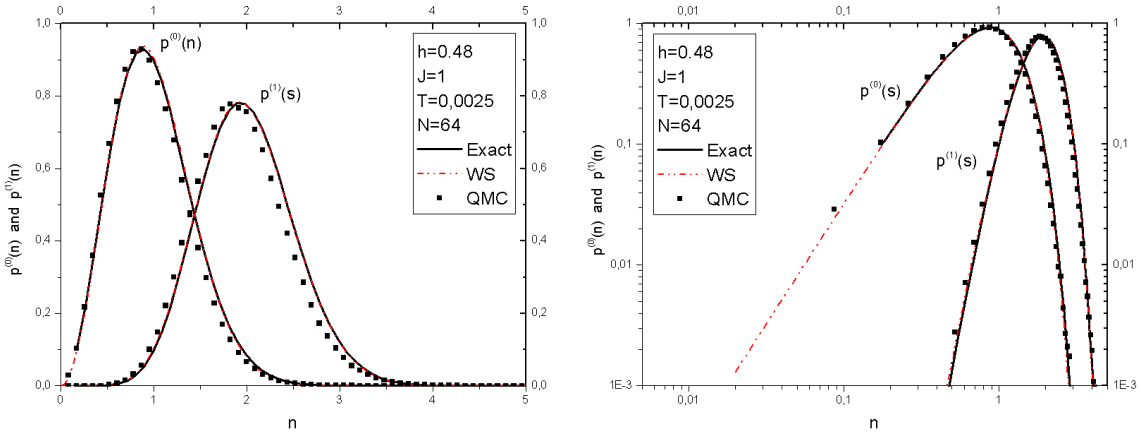

Figure **5-7**: Normalized p_n^0 and p_n^1 spacing-distributions for a chain of size N=64, h=0.48 and T=0.0025.

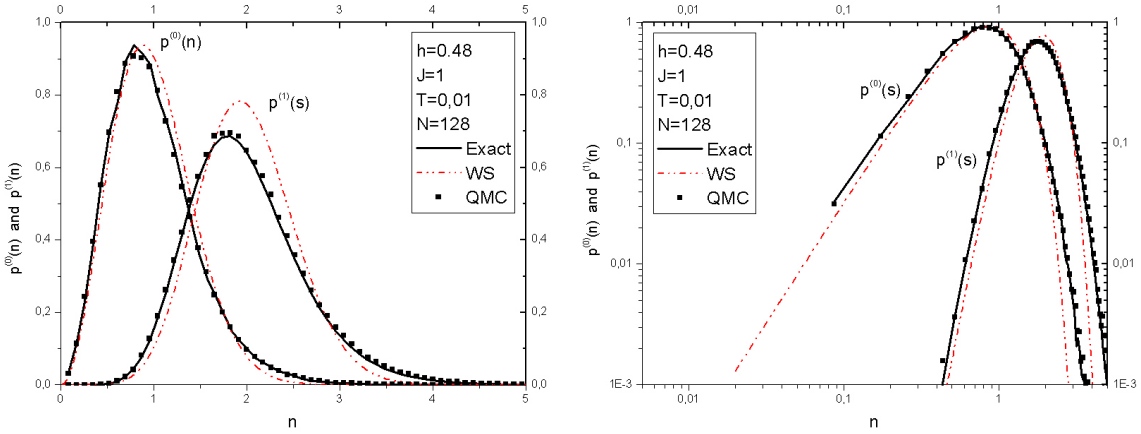

Figure **5-8**: Normalized p_n^0 and p_n^1 spacing-distributions for a chain of size N=128, h=0.48 and T=0.01.

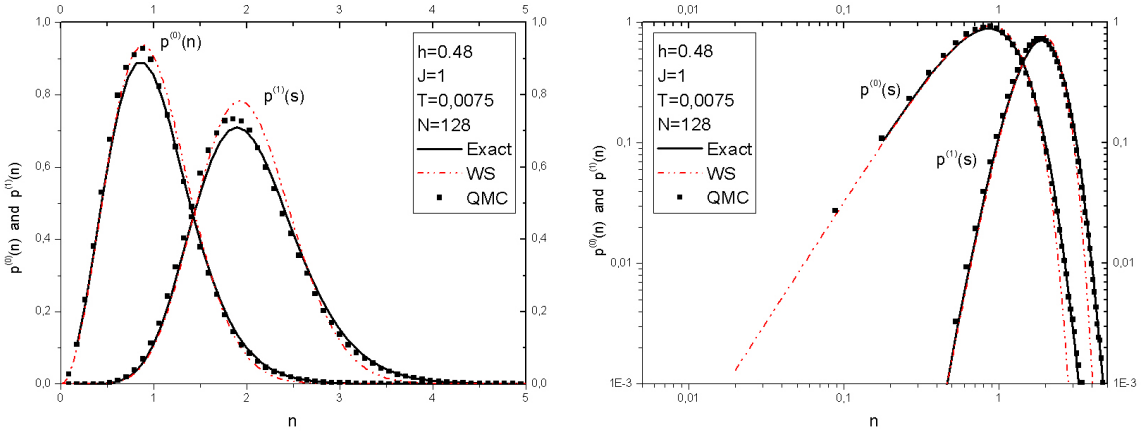

Figure **5-9**: Normalized p_n^0 and p_n^1 spacing-distributions for a chain of size N=128, h=0.48 and T=0.0075.

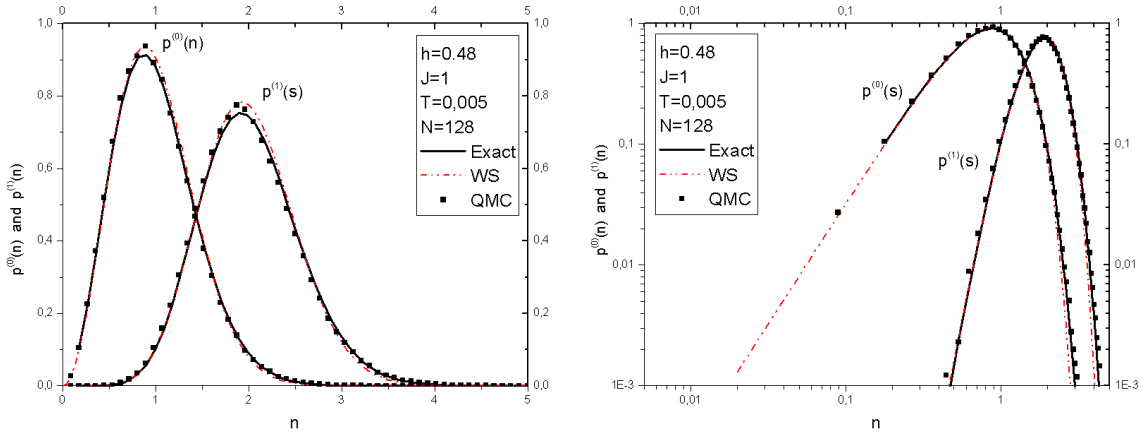

Figure **5-10**: Normalized p_n^0 and p_n^1 spacing-distributions for a chain of size N=128, h=0.48 and T=0.005.

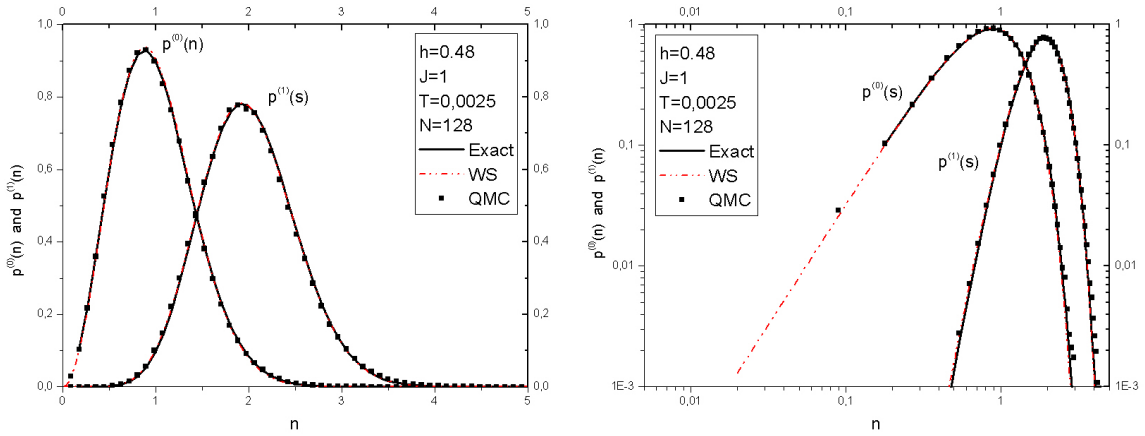

Figure **5-11**: Normalized p_n^0 and p_n^1 spacing-distributions for a chain of size N=128, h=0.48 and T=0.0025.

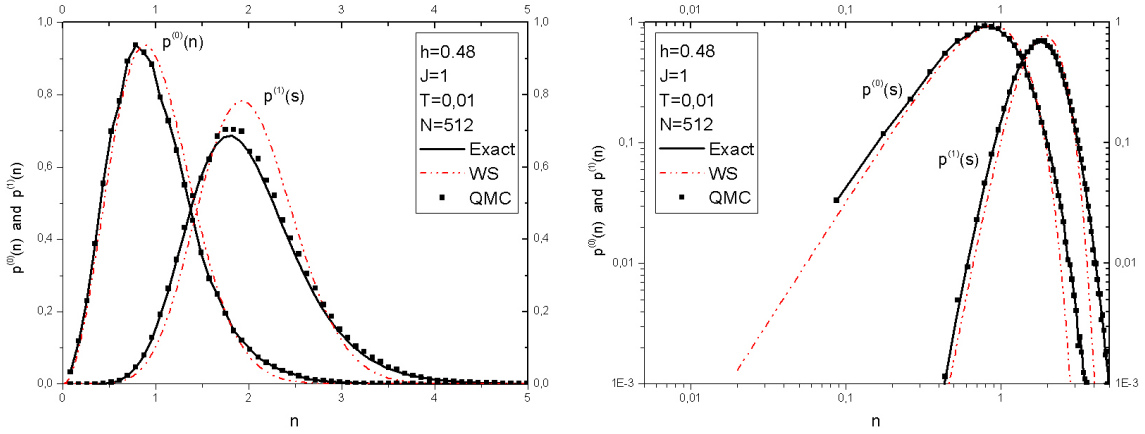

Figure **5-12**: Normalized p_n^0 and p_n^1 spacing-distributions for a chain of size N=512, h=0.48 and T=0.01.

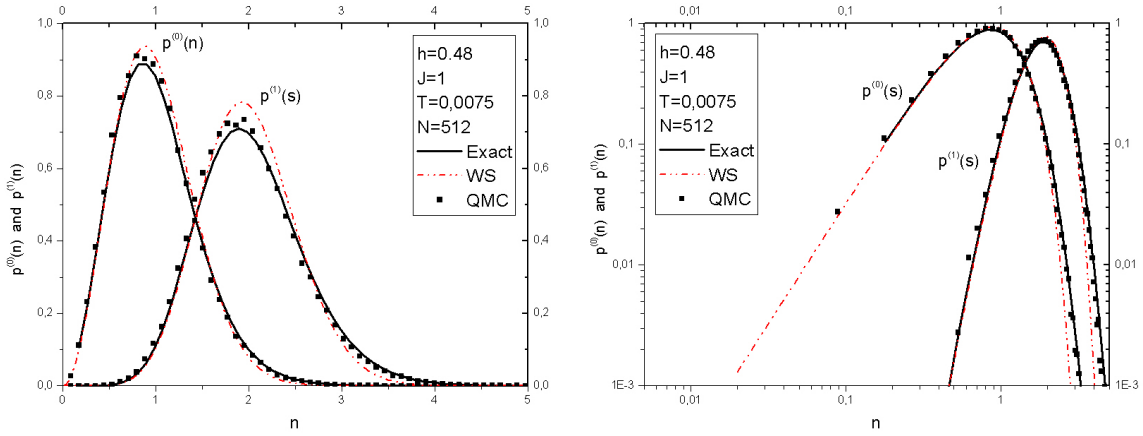

Figure **5-13**: Normalized p_n^0 and p_n^1 spacing-distributions for a chain of size N=512, h=0.48 and T=0.0075.

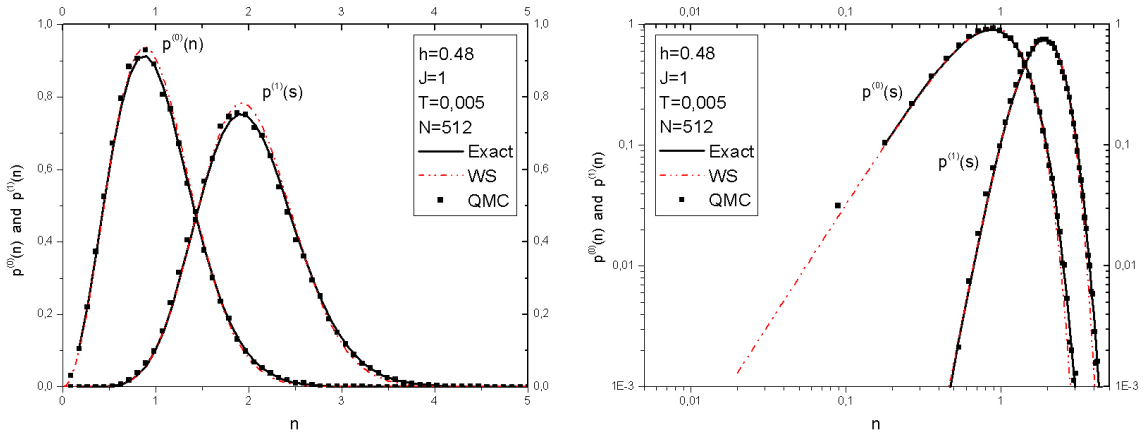

Figure **5-14**: Normalized p_n^0 and p_n^1 spacing-distributions for a chain of size N=512, h=0.48 and T=0.005.

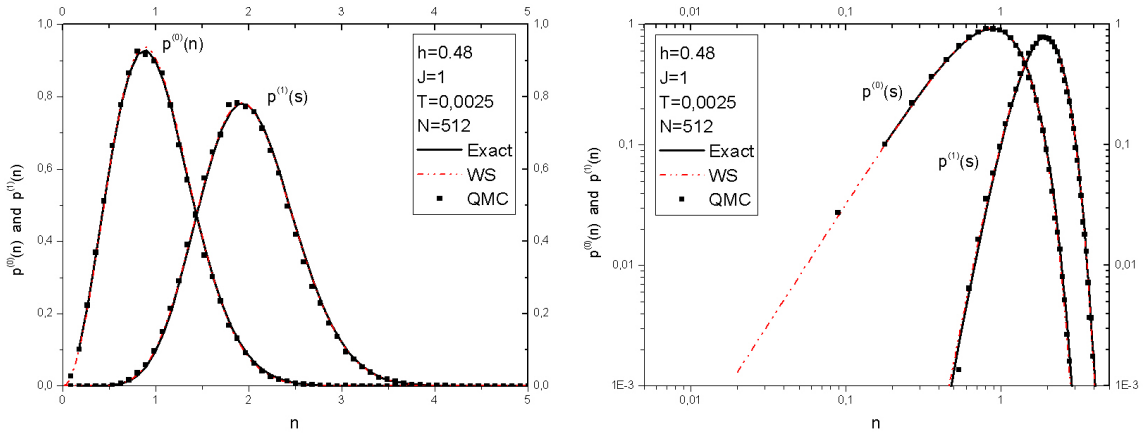

Figure **5-15**: Normalized p_n^0 and p_n^1 spacing-distributions for a chain of size N=512, h=0.48 and T=0.0025.

Chapter 6

Summary and outlook

The XX spin chain in the presence of a magnetic field h is an integrable system and one of the simplest quantum systems displaying long-range correlations along with the associated large fluctuations. Therefore, it is a good starting point to begin the study interacting many-particle systems. We present in detail the procedure required to diagonalized Hamiltonian, the calculation of the partition function and some thermodynamic observables.

The best-known correlation function, EFP $P(n)$, was presented and based on its representation as a Toeplitz determinant was showed its asymptotic behavior for large and small values of n. One of the main results if the fact that $P(n)$ presents a Gaussian decay for zero-temperature and exponential decay for finite-temperature.

For the regime $h \to J/2$ we calculate the spacing distributions p_n^0 and p_n^1. The equivalence between the IPDF method and the fermion formalism is illustrated and discussed. The GWS is compared with our numerical and analytical results showing an excellent agreement.

The SSE QMC method was implemented successfully, the computational simulations reproduced satisfactorily the thermodynamic observables despite we use a small system (N=64) and few iterations to reach the equilibrium (80000 MCS). For the spacing-distributions we performed an extensive simulation (500000 MCS) for several system sizes (N=64, 128 and 512) and different temperatures (T=0.01, 0.0075, 0.005 and 0.0025) with a fixed magnetic field (h=0.48). For the lowest temperature considered, the analytical results fit really nice to the QMC simulation and the GWS approximation. As expected, for higher temperatures, the behavior of spacing-distribution deviates from the GWS but the analytical and computational results always agree.

Appendix A

Jordan-Wigner transformation (JWT)

The XX model can be diagonalized using a more convenient representation. In the JWT, the interacting spin system is mapped onto an non-interacting fermion system, which can be easily diagonalized in the momentum space by using the Fourier transform [66].

The JWT is defined through the operators $\hat{c}_j$ and $\hat{c}_j^\dagger$ according to

$$\hat{c}_j = e^{i\pi \sum_{k=1}^{j-1} \hat{S}_k^- \hat{S}_k^+} \hat{S}_j^+, \quad \text{and} \quad \hat{c}_j^\dagger = \hat{S}_j^- e^{-i\pi \sum_{k=1}^{j-1} \hat{S}_k^- \hat{S}_k^+}. \tag{A-1}$$

It is easy to see that the corresponding inverse transformation is given by

$$\begin{aligned} \hat{S}_j^+ &= e^{-i\pi \sum_{k=1}^{j-1} \hat{c}_k^\dagger \hat{c}_k} \hat{c}_j = \prod_{k=1}^{j-1} \left(1 - 2\hat{c}_k^\dagger \hat{c}_k\right) \hat{c}_j, \quad \text{and} \\ \hat{S}_j^- &= \hat{c}_j^\dagger e^{i\pi \sum_{k=1}^{j-1} \hat{c}_k^\dagger \hat{c}_k} = \hat{c}_j^\dagger \prod_{k=1}^{j-1} \left(1 - 2\hat{c}_k^\dagger \hat{c}_k\right). \end{aligned} \tag{A-2}$$

The action of the $\hat{c}_j$ operator over the eigenstates of $\hat{S}_j^z$ can be calculated as follows

$$\begin{aligned} \hat{c}_j \left|\cdots \downarrow \cdots\right\rangle &= e^{i\pi \sum_{k=1}^{j-1} \hat{S}_k^- \hat{S}_k^+} \hat{S}_j^+ \left|\cdots \downarrow \cdots\right\rangle \\ &= e^{i\pi \sum_{k=1}^{j-1} \hat{S}_k^- \hat{S}_k^+} \left|\cdots \uparrow \cdots\right\rangle \\ &= e^{i\pi M_j} \left|\cdots \uparrow \cdots\right\rangle, \end{aligned} \tag{A-3}$$

where M_j denotes the number of spins pointing up at the left of the jth spin. Similarly, for the other eigenstate we have

$$\hat{c}_j \left|\cdots \uparrow \cdots\right\rangle = e^{i\pi \sum_{j=1}^{k-1} \hat{S}_j^- \hat{S}_j^+} \hat{S}_j^+ \left|\cdots \uparrow \cdots\right\rangle = 0 \tag{A-4}$$

where in both, Eqs. (A-3) and (A-4) we have used the Eqs. (1-12). For the $\hat{c}_j^\dagger$ operator the calculation is complete analogous, so we obtain

$$\hat{c}_j^\dagger \left|\cdots\uparrow\cdots\right\rangle = e^{-i\pi M_j} \left|\cdots\downarrow\cdots\right\rangle, \tag{A-5}$$

and

$$\hat{c}_j^\dagger \left|\cdots\downarrow\cdots\right\rangle = 0, \tag{A-6}$$

where we have used the Eqs. (1-11).

A.1 Algebra of the Jordan-Wigner operators

The new operators satisfies the following relations

$$\hat{c}_j^\dagger \hat{c}_j = \hat{S}_j^- e^{-i\pi\sum_{k=1}^{j-1}\hat{S}_k^-\hat{S}_k^+} e^{i\pi\sum_{k=1}^{j-1}\hat{S}_k^-\hat{S}_k^+}\hat{S}_j^+ = \hat{S}_j^-\hat{S}_j^+, \tag{A-7}$$

and

$$\hat{c}_j\hat{c}_j^\dagger = e^{i\pi\sum_{k=1}^{j-1}\hat{S}_k^+\hat{S}_k^-}\hat{S}_j^+\hat{S}_j^- e^{-i\pi\sum_{k=1}^{j-1}\hat{S}_k^-\hat{S}_k^+} = \hat{S}_j^+\hat{S}_j^-, \tag{A-8}$$

where we have taken into account that for different sites the following relation

$$[\hat{S}_j^\pm, f(\hat{S}_k^+, \hat{S}_k^-)] = 0, \quad \text{for} \quad j \neq k, \tag{A-9}$$

where $f(\hat{S}_j^+, \hat{S}_j^-)$ denotes an arbitrary function of the operators $\hat{S}_j^+$ and $\hat{S}_j^-$. Using the Eqs. (A-7) and (A-8) we can conclude that

$$\{\hat{c}_j^\dagger, \hat{c}_j\} = \{\hat{S}_j^-, \hat{S}_j^+\} = \hat{I}. \tag{A-10}$$

Now, we will consider the case where the operators act on different sites $j \neq k$. Two different scenarios has to be considered, for $j > k$ we have

$$\begin{aligned}\hat{c}_j^\dagger\hat{c}_k &= \hat{S}_j^- e^{-i\pi\sum_{l=1}^{j-1}\hat{S}_l^+\hat{S}_l^-} e^{i\pi\sum_{l'=1}^{k-1}\hat{S}_{l'}^+\hat{S}_{l'}^-}\hat{S}_k^+ \\ &= \hat{S}_j^-\hat{S}_k^+ e^{-i\pi\sum_{l=k+1}^{j-1}(\hat{S}_l^+\hat{S}_l^-)}\end{aligned} \tag{A-11}$$

Following the same procedure to find Eq. (A-11), it is easy to show that

$$\hat{c}_k\hat{c}_j^\dagger = \hat{S}_k^+\hat{S}_j^- e^{-i\pi\sum_{l=k+1}^{j-1}(\hat{S}_l^+\hat{S}_l^-)}. \tag{A-12}$$

Therefore, from Eqs. (A-11) and (A-12) we conclude that for $j > k$ we have

$$\{\hat{c}_j^\dagger, \hat{c}_k\} = \{\hat{S}_j^+, \hat{S}_k^-\} e^{-i\pi\sum_{l=k+1}^{j-1}(\hat{S}_l^+\hat{S}_l^-)} = \hat{I}\delta_{jk}. \tag{A-13}$$

The proof for the case $j < k$ is quite similar, and is not difficult to see that

$$\{\hat{c}_k^\dagger, \hat{c}_j\} = \{\hat{S}_k^+, \hat{S}_j^-\} e^{-i\pi \sum_{l=k+1}^{j-1} (\hat{S}_l^+ \hat{S}_l^-)} = \hat{I}\delta_{kj}. \tag{A-14}$$

Because the Kronecker delta is a symmetric tensor we can conclude that Eq. (A-13) and Eq. (A-14) are satisfied for all values of j and k. Now we can write the algebra for the operators defined by the JWT using Eq. (A-10) and (A-13), obtaining

$$\{\hat{c}_j^\dagger, \hat{c}_k\} = \hat{I}\delta_{jk} \quad \text{and} \quad \{\hat{c}_j^\dagger, \hat{c}_k^\dagger\} = \{\hat{c}_j, \hat{c}_k\} = 0. \tag{A-15}$$

The proof of the last relation is straightforward and it is not included in the text. We conclude that the $\hat{c}_j^\dagger$ and $\hat{c}_j$ operators obey the canonical fermion algebra. Note that we have defined the transformation (A-1) such as a spin-down is equivalent to a fermion, and a spin-up to a empty site.

Appendix B

Generalized Wigner surmise (GWS) for spacing-distributions

B.1 Brief overview of the Wigner surmise

The spacing distributions of Gaussian and Circular ensembles of random matrices are well described by the Wigner surmise (WS). The WS provides simple and easy to use expression for p_n^m. In this section we summarize its most important properties. The symmetry properties define the degree of level repulsion in the energy spectrum of the ensemble, i.e., determine the behavior of the distribution for small spacing values. The behavior of the nearest-neighbor-spacing distribution for small values of the spacing behave as follows

$$P_\beta(s) \propto s^\beta, \quad \text{for} \quad s \to 0, \tag{B-1}$$

where $\beta = 1$ for the Gaussian Orthogonal Ensemble GOE, $\beta = 2$ for the Gaussian Unitary Ensemble GUE and $\beta = 4$ for Gaussian Symplectic Ensemble GSE. The Gaussian distribution of the Hamiltoninan matrix elements suggest a Gaussian tail for $P_\beta(s)$ at large s. Therefore, a reasonable approximation for $P(s)$ is given by

$$P_\beta(s) = A_\beta s^\beta e^{-B_\beta s^2}, \tag{B-2}$$

where A_β and B_β are obtained from the normalization condition and the requirement that the mean spacing is unity, respectively. This is the Wigner surmise for random matrices [41]. Explicitly, for the particular case GUE the normalization constants have the simple form

$$A_2 = \frac{32}{\pi^2}, \quad \text{and} \quad B_2 = \frac{4}{\pi}. \tag{B-3}$$

The WS is an exact result just for ensembles of 2×2 matrices but it is an excellent approximation for $N \times N$ matrices.

B.2 High-order level spacing distribution

In 1998 A. Y. Abul-Magd and M. H. Simbel proposed an extension of the WS to describe the nth-order spacing distributions [67]. Their main assumption is that the occurrence of consecutive levels in a chaotic system is a random process. This suggest to express the conditional probability $r_\beta(n,s)$ of the occurrence of the $(n+1)$th level at a distance s as follows

$$r_\beta(n,s) \propto s^{(n+1)\beta}, \quad \text{for} \quad s \to 0. \tag{B-4}$$

Therefore, for small values of s the n-th can be written as

$$P_\beta(n,s) = c_n\, s^{(n+1)\beta} \int_0^s P_\beta(n-1,x)dx \tag{B-5}$$

where c_n is a constant. Solving previous equation recursively, it is easy to obtain

$$P_\beta(n,s) \propto s^{\alpha_{\beta,n}}, \quad \text{for} \quad s \to 0, \tag{B-6}$$

where

$$\alpha_{\beta,n} = n + \frac{(n+1)(n+2)}{2}\beta. \tag{B-7}$$

Finally, assuming that the tail of $P_\sigma(n,s)$ for large values of s is Gaussian, it is possible to find the following generalization of the WS

$$P_\beta(n,s) = A_{\beta,n} s^{\alpha_{\beta,n}} \exp\left(-B_{\beta,n}s^2\right). \tag{B-8}$$

As before, the constants $A_{\beta,n}$ and $B_{\beta,n}$ are obtained from the normalization conditions.

$$\int_0^\infty P_\beta(n,s)ds = 1 \quad \text{and} \quad \int_0^\infty sP_\beta(n,s)ds = n+1. \tag{B-9}$$

The explicit form of the conditions are

$$A_{\beta,n} = \frac{2B_{\beta,n}^{(\alpha_{\beta,n}+1)/2}}{\Gamma\left(\frac{\alpha_{\beta,n}+1}{2}\right)} \quad \text{and} \quad B_{\beta,n} = \left[\frac{\Gamma\left(\frac{\alpha_{\beta,n}}{2}+1\right)}{(n+1)\Gamma\left(\frac{\alpha_{\beta,n}+1}{2}\right)}\right]^2. \tag{B-10}$$

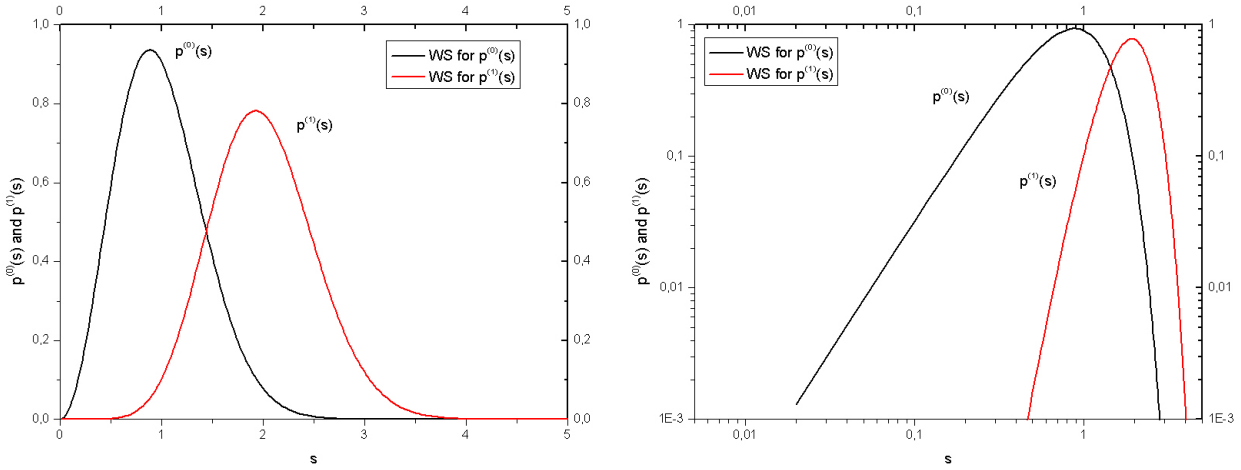

Figure **B-1**: Wigner surmise for the $p^{(0)}(s)$ and $p^{(1)}(s)$ spacing-distributions. The left graph is useful to see the behavior of the spacing-distributions for large values of s and the Gaussian decay. The right graph shows the same GWS but with logarithmic scale, in order to see clearly the behavior of the spacing-distributions for small values of s.

Appendix C

Probabilities used in loop update

In the following list we present the probabilities used in the loop update step, this information is stored in a static 3-dimensional array p[7][4][4], remember that in C++ the array indexing starts from 0. The first element represents the vertex type, 6 in this case, in order to simplify the memory access in the algorithm we define the first array element as 7 and not 6. In this way we can list the vertex types from 1 to 6 instead of 0 to 5. The second and third element of the arrays represent the "entrance" and "exit" legs, respectively, we list the legs from 0 to 3 so we have no problems in this case.

In the code implementation we use the following notation for each probability

$$p1 = \mathcal{A}_{insert}^{(6)} \tag{C-1}$$
$$p2 = \mathcal{A}_{insert}^{(1)} \tag{C-2}$$
$$p3 = \mathcal{A}_{insert}^{(2,3)} \tag{C-3}$$
$$p4 = \mathcal{A}_{insert}^{(4,5)} \tag{C-4}$$

In the list we indicate the corresponding process to each probability, so the processes are denoted as follows

- Bounce: B
- Continue straight: St
- Switch and continue: SC
- Switch and reverse: SR

The probabilities associated to a given process will not always be the same, for example, depending on 1-type vertex, a bounce process will be represented by p1, but for another type of vertex this is no longer true. The procedure to associate the probabilities is quite simple, given one of the six possible vertices we choose the entrance leg and select the exit leg, and flip the two corresponding spins, depending on the resultant spin configuration we determine the new vertex. For a given vertex there are 16 different enter and exit combinations, and there are 6 types of vertices, obtaining in total 96 probabilities/processes.

The following list uses the syntax of a C ++ code, so it can be directly copied and pasted for use.

```
p[1][0][0] = p1; /*B*/  p[1][0][1] = 0;
p[1][0][3] = p4; /*SC*/ p[1][0][2] = p3; /*St*/

p[1][1][0] = 0;         p[1][1][1] = p1; /*B*/
p[1][1][3] = p3; /*St*/ p[1][1][2] = p4; /*SC*/

p[1][3][0] = p4; /*SC*/ p[1][3][1] = p3; /*St*/
p[1][3][3] = p1; /*B*/  p[1][3][2] = 0;

p[1][2][0] = p3; /*St*/ p[1][2][1] = p4; /*SC*/
p[1][2][3] = 0;         p[1][2][2] = p1; /*B*/

/*----------------------------------------*/

p[2][0][0] = p3; /*B*/  p[2][0][1] = p4; /*SR*/
p[2][0][3] = 0;         p[2][0][2] = p2; /*St*/

p[2][1][0] = p4; /*SR*/ p[2][1][1] = p3; /*B*/
p[2][1][3] = p1; /*St*/ p[2][1][2] = 0;

p[2][3][0] = 0;         p[2][3][1] = p1; /*St*/
p[2][3][3] = p3; /*B*/  p[2][3][2] = p4; /*SR*/

p[2][2][0] = p2; /*St*/ p[2][2][1] = 0;
p[2][2][3] = p4; /*SR*/ p[2][2][2] = p3; /*B*/

/*----------------------------------------*/

p[3][0][0] = p3; /*B*/  p[3][0][1] = p4; /*SR*/
p[3][0][3] = 0;         p[3][0][2] = p1; /*St*/

p[3][1][0] = p4; /*SR*/ p[3][1][1] = p3; /*B*/
p[3][1][3] = p2; /*St*/ p[3][1][2] = 0;

p[3][3][0] = 0;         p[3][3][1] = p2; /*St*/
p[3][3][3] = p3; /*B*/  p[3][3][2] = p4; /*SR*/

p[3][2][0] = p1; /*St*/ p[3][2][1] = 0;
p[3][2][3] = p4; /*SR*/ p[3][2][2] = p3; /*B*/

/*----------------------------------------*/

p[4][0][0] = p4; /*B*/  p[4][0][1] = p3; /*SR*/
p[4][0][3] = p2; /*SC*/ p[4][0][2] = 0;
```

```
p[4][1][0] = p3; /*SR*/ p[4][1][1] = p4; /*B*/
p[4][1][3] = 0;         p[4][1][2] = p1; /*SC*/

p[4][3][0] = p2; /*SC*/ p[4][3][1] = 0;
p[4][3][3] = p4; /*B*/  p[4][3][2] = p3; /*SR*/

p[4][2][0] = 0;         p[4][2][1] = p1; /*SC*/
p[4][2][3] = p3; /*SR*/ p[4][2][2] = p4; /*B*/

/*----------------------------------------*/

p[5][0][0] = p4; /*B*/  p[5][0][1] = p3; /*SR*/
p[5][0][3] = p1; /*SC*/ p[5][0][2] = 0;

p[5][1][0] = p3; /*SR*/ p[5][1][1] = p4; /*B*/
p[5][1][3] = 0;         p[5][1][2] = p2; /*SC*/

p[5][3][0] = p1; /*SC*/ p[5][3][1] = 0;
p[5][3][3] = p4; /*B*/  p[5][3][2] = p3; /*SR*/

p[5][2][0] = 0;         p[5][2][1] = p2; /*SC*/
p[5][2][3] = p3; /*SR*/ p[5][2][2] = p4; /*B*/

/*----------------------------------------*/

p[6][0][0] = p2; /*B*/  p[6][0][1] = 0;
p[6][0][3] = p4; /*SC*/ p[6][0][2] = p3; /*St*/

p[6][1][0] = 0;         p[6][1][1] = p2; /*B*/
p[6][1][3] = p3; /*St*/ p[6][1][2] = p4; /*SC*/

p[6][3][0] = p4; /*SC*/ p[6][3][1] = p3;
p[6][3][3] = p2; /*B*/  p[6][3][2] = 0;

p[6][2][0] = p3; /*St*/ p[6][2][1] = p4; /*SC*/
p[6][2][3] = 0;         p[6][2][2] = p2; /*B*/
```

Appendix D

Linked vertex list

The linked vertex representation contains the complete information about the way the operators are connected. Therefore, it is possible to perform a directly jump from the “exit’ ’ leg of an operator at the time slice p, which acts on two spins at bond b to the “entrance’ ’ leg of the next or previous operator acting on one of these spins. It worth note that there is no need to perform a rigorous search in the list opstring[] [3].

In the case of the isotropic Heisenberg model, there are four allowed vertices, see Figure **D-1**. Anisotropic interactions and external magnetic fields require the inclusion of additional vertices [2, 28] as was shown in chapter 4. The open and solid bars in the figure **D-1** represent diagonal and off-diagonal vertices, respectively. Note that a vertex can be identified uniquely by the spin states at the four legs.

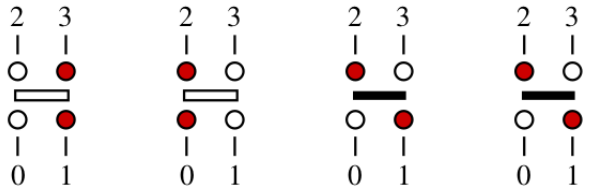

Figure **D-1**: Allowed vertices for the isotropic spin-1/2 Heisenberg model. The numbering $l = 0,\ 1,\ 2,\ 3$ of the vertex legs corresponds to the position $v = 4p + l$, in linked-list storage. This figure appears as Fig. 58 in [3].

A graphical representation of the vertex list, for a particular configuration, is shown in Fig. **4-2**.

For a given timeslice p, the corresponding list element $s(p)$ returns the operator type (diagonal or off-diagonal) and the bond b on which it acts. Along with this information, we only must store the connectivity of the vertices, therefore there is no need to save the respective spin states. The links among the connected vertex legs are stored as a list $X(v)$. The list in figure **D-2** has been arranged in four columns, with elements labelled $v = 4p + l$, corresponding to each type of leg, $l = 0, 1, 2, 3$, and the labelling specified in Fig. **D-1**.

Is sufficient to know that for a given operator at p, the position of its l-th leg in the linked vertex list is $v = 4\,p + l$. This leg is linked to another vertex leg with list address $v' = X(v)$. Note that $X[X(v)] = v$, this kind of structure is known as a doubly-linked (bi-directional) list.

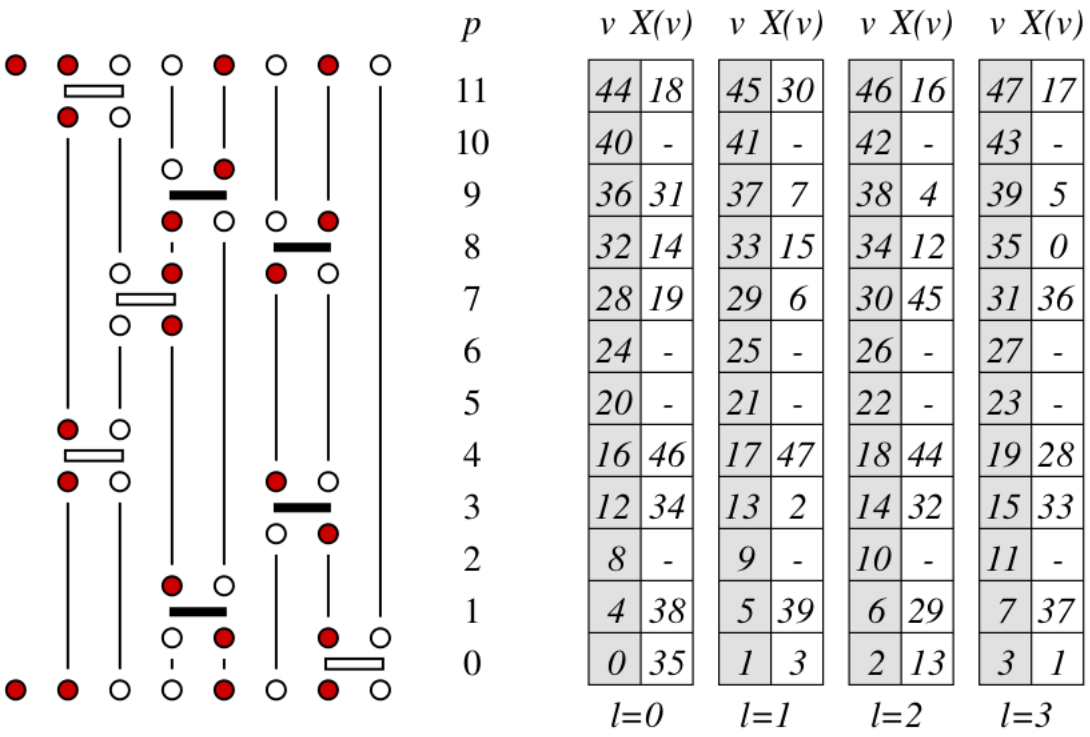

Figure **D-2**: Linked vertex storage of the configuration shown in Fig. **4-2**. In the graphical representation to the left, constant spin states between operators have been replaced by lines (links) connecting the spins just before and after the operator acts. The links can be stored in a list $X(v)$, where the four elements $v = 4p + l$, $l = 0, 1, 2, 3$, correspond to the legs of the vertex at position p. For two linked legs v and v', $X(v) = v'$ and $X(v') = v$. This figure appears as Fig. 58 in [3].

Note that for a given position v in the list we can extract the corresponding operator location, $p = v/4$ (only consider its integer part) and leg index $l = mod(v, 4)$. We can move to the other leg on the same vertex by changing the leg label $0 \leftrightarrow 1$ or $2 \leftrightarrow 3$. These movements allow us to construct closed loops.

Bibliography

[1] A. W. Sandvik, "Computational studies of quantum spin systems," *AIP Conference Proceedings*, vol. 1297, no. 1, pp. 135–338, 2010.

[2] O. Syljuåsen and A. Sandvik, "Quantum monte carlo with directed loops," *Physical review. E, Statistical, nonlinear, and soft matter physics*, vol. 66, p. 046701, 11 2002.

[3] A. W. Sandvik and J. Kurkijärvi, "Quantum monte carlo simulation method for spin systems," *Phys. Rev. B*, vol. 43, pp. 5950–5961, Mar 1991.

[4] F. Franchini, *An Introduction to Integrable Techniques for One-Dimensional Quantum Systems*, vol. 940. 09 2016.

[5] V. E. Korepin, N. M. Bogoliubov, and A. G. Izergin, *Quantum Inverse Scattering Method and Correlation Functions*. Cambridge Monographs on Mathematical Physics, Cambridge University Press, 1993.

[6] M. Jimbo and T. Miwa, "Algebraic analysis of solvable lattice models.," 1994.

[7] M. Takahashi, *Thermodynamics of One-Dimensional Solvable Models*. Cambridge University Press, 1999.

[8] W. Heisenberg, "Zur theorie des ferromagnetismus," *Zeitschrift für Physik*, vol. 49, 09 1928.

[9] J. Levy, "Universal quantum computation with spin- 1 / 2 pairs and heisenberg exchange," *Physical review letters*, vol. 89, p. 147902, 10 2002.

[10] P. Estarellas, "Spin chain systems for quantum computing and quantum information applications," 2018.

[11] S. Bose, "Quantum communication through an unmodulated spin chain," *Physical Review Letters*, vol. 91, Nov 2003.

[12] S. Bose, "Quantum communication through spin chain dynamics: an introductory overview," *Contemporary Physics*, vol. 48, p. 13–30, Jan 2007.

[13] D. Petrosyan, G. M. Nikolopoulos, and P. Lambropoulos, "State transfer in static and dynamic spin chains with disorder," *Physical Review A*, vol. 81, Apr 2010.

[14] N. Y. Yao, L. Jiang, A. V. Gorshkov, Z.-X. Gong, A. Zhai, L.-M. Duan, and M. D. Lukin, "Robust quantum state transfer in random unpolarized spin chains," *Phys. Rev. Lett.*, vol. 106, p. 040505, Jan 2011.

[15] H. Schwager, J. I. Cirac, and G. Giedke, "Dissipative spin chains: Implementation with cold atoms and steady-state properties," *Physical Review A*, vol. 87, Feb 2013.

[16] O. V. Marchukov, A. G. Volosniev, M. Valiente, D. Petrosyan, and N. T. Zinner, "Quantum spin transistor with a heisenberg spin chain," *Nature Communications*, vol. 7, Oct 2016.

[17] M. Shiroishi, M. Takahashi, and Y. Nishiyama, "Emptiness formation probability for the one-dimensional isotropic xy model," *Journal of the Physical Society of Japan*, vol. 70, 06 2001.

[18] V. E. Korepin, A. G. Izergin, F. H. Essler, and D. B. Uglov, "Correlation function of the spin-12 xxx antiferromagnet," *Physics Letters A*, vol. 190, no. 2, pp. 182 – 184, 1994.

[19] F. H. Essler, H. Frahm, A. R. Its, and V. E. Korepin, "Integro-difference equation for a correlation function of the spin-12 heisenberg xxz chain," *Nuclear Physics B*, vol. 446, no. 3, pp. 448 – 460, 1995.

[20] N. Kitanine, J. Maillet, and V. Terras, "Correlation functions of the xxz heisenberg spin-12 chain in a magnetic field," *Nuclear Physics B*, vol. 567, no. 3, pp. 554 – 582, 2000.

[21] M. Jimbo and T. Miwa, "Quantum KZ equation with $|q| = 1$ and correlation functions of theXXZmodel in the gapless regime," *Journal of Physics A: Mathematical and General*, vol. 29, pp. 2923–2958, jun 1996.

[22] D. ben Avraham and S. Havlin, *Diffusion and Reactions in Fractals and Disordered Systems*. Cambridge University Press, 2000.

[23] J. G. Amar and F. Family, "Diffusion annihilation in one dimension and kinetics of the ising model at zero temperature," *Phys. Rev. A*, vol. 41, pp. 3258–3262, Mar 1990.

[24] P. Argyrakis and R. Kopelman, "Nearest-neighbor distance distributions and self-ordering in diffusion-controlled reactions. i. a+a simulations," *Phys. Rev. A*, vol. 41, pp. 2114–2120, Feb 1990.

[25] A. Faggionato, F. Martinelli, C. Roberto, and C. Toninelli, "Universality in one-dimensional hierarchical coalescence processes," *The Annals of Probability*, vol. 40, p. 1377–1435, Jul 2012.

[26] D. ben Avraham and S. Havlin, *Diffusion and Reactions in Fractals and Disordered Systems*. Cambridge University Press, 2000.

[27] M. Suzuki, "Relationship between d-Dimensional Quantal Spin Systems and (d+1)-Dimensional Ising Systems: Equivalence, Critical Exponents and Systematic Approximants of the Partition Function and Spin Correlations," *Progress of Theoretical Physics*, vol. 56, pp. 1454–1469, 11 1976.

[28] A. W. Sandvik, "Stochastic series expansion method with operator loop update," *Phys. Rev. B*, vol. 59, p. 14157, 1999.

[29] L. Faddeev, N. Reshetikhin, and L. Takhtajan, "Quantization of Lie Groups and Lie Algebras," *Alg. Anal.*, vol. 1, no. 1, pp. 178–206, 1989.

[30] L. Faddeev and L. Takhtajan, "What is the spin of a spin wave?," *Phys. Lett. A*, vol. 85, pp. 375–377, 1981.

[31] L. Faddeev, "From integrable models to quantum groups," in *29th International Universitatswochen fur Kernphysik (International University School of Particle Physics: Fields and Particles)*, pp. 89–115, 1990.

[32] L. A. Takhtajan, *Lectures on Quamtum Groups*, pp. 69–197.

[33] L. D. Faddeev, "How algebraic bethe ansatz works for integrable model," 1996.

[34] L. FADDEEV, "Algebraic aspects of the bethe ansatz," *International Journal of Modern Physics A*, vol. 10, p. 1845–1878, May 1995.

[35] E. K. Sklyanin, "Quantum inverse scattering method. selected topics," 1992.

[36] T. Deguchi, "Introduction to solvable lattice models in statistical and mathematical physics," *Classical and Quantum Nonlinear Integrable System*.

[37] A. Klümper, "Integrability of quantum chains: Theory and applications to the spin-1/2 xxz chain," *Lecture Notes in Physics*, p. 349–379, 2004.

[38] P. W. Anderson, "New approach to the theory of superexchange interactions," *Phys. Rev.*, vol. 115, pp. 2–13, Jul 1959.

[39] A. Zee, *Group Theory in a Nutshell for Physicists*. In a Nutshell, Princeton University Press, 2016.

[40] A. Doikou, S. Evangelisti, G. Feverati, and N. Karaiskos, "Introduction to quantum integrability," *International Journal of Modern Physics A*, vol. 25, 12 2009.

[41] M. L. Mehta, *Random Matrices*. Elsevier Academic Press, third ed., 2004.

[42] H. Widom and M. Kac, "The strong szegö limit theorem for circular arcs," *Indiana University Mathematics Journal*, vol. 21, no. 3, pp. 277–283, 1971.

[43] T. Wu and B. M. McCoy, *The two-dimensional Ising model*. Harvard University Press, first ed., 1973.

[44] C. R. Doering and D. ben Avraham, "Interparticle distribution functions and rate equations for diffusion-limited reactions," *Phys. Rev. A*, vol. 38, pp. 3035–3042, Sep 1988.

[45] R. P. Feynman, "Atomic theory of the λ transition in helium," *Phys. Rev.*, vol. 91, pp. 1291–1301, Sep 1953.

[46] J. E. Hirsch, R. L. Sugar, D. J. Scalapino, and R. Blankenbecler, "Monte carlo simulations of one-dimensional fermion systems," *Phys. Rev. B*, vol. 26, pp. 5033–5055, Nov 1982.

[47] M. Suzuki, "Relationship between d-Dimensional Quantal Spin Systems and (d+1)-Dimensional Ising Systems: Equivalence, Critical Exponents and Systematic Approximants of the Partition Function and Spin Correlations," *Progress of Theoretical Physics*, vol. 56, pp. 1454–1469, 11 1976.

[48] M. Suzuki, S. Miyashita, and A. Kuroda, "Monte Carlo Simulation of Quantum Spin Systems. I," *Progress of Theoretical Physics*, vol. 58, pp. 1377–1387, 11 1977.

[49] B. B. Beard and U.-J. Wiese, "Simulations of discrete quantum systems in continuous euclidean time," *Phys. Rev. Lett.*, vol. 77, pp. 5130–5133, Dec 1996.

[50] D. C. Handscomb, "The monte carlo method in quantum statistical mechanics," *Mathematical Proceedings of the Cambridge Philosophical Society*, vol. 58, no. 4, p. 594–598, 1962.

[51] D. C. Handscomb, "A monte carlo method applied to the heisenberg ferromagnet," *Mathematical Proceedings of the Cambridge Philosophical Society*, vol. 60, no. 1, p. 115–122, 1964.

[52] J. W. Lyklema, "Quantum-statistical monte carlo method for heisenberg spins," *Phys. Rev. Lett.*, vol. 49, pp. 88–90, Jul 1982.

[53] D. H. Lee, J. D. Joannopoulos, and J. W. Negele, "Monte carlo solution of antiferromagnetic quantum heisenberg spin systems," *Phys. Rev. B*, vol. 30, pp. 1599–1602, Aug 1984.

[54] "Monte carlo study of the two-dimensional spin-1/2 quantum heisenberg model: Spin correlations in la_2cuo_4, author = Manousakis, Efstratios and Salvador, Román, journal = Phys. Rev. B, volume = 39, issue = 1, pages = 575–585, numpages = 0, year = 1989, month = Jan, publisher = American Physical Society, doi = 10.1103/PhysRevB.39.575, url = https://link.aps.org/doi/10.1103/PhysRevB.39.575,"

[55] S. Chakravarty and D. B. Stein, "Monte carlo simulation of quantum spin systems," *Phys. Rev. Lett.*, vol. 49, pp. 582–585, Aug 1982.

[56] A. W. Sandvik, "Stochastic series expansion method with operator-loop update," *Phys. Rev. B*, vol. 59, pp. R14157–R14160, Jun 1999.

[57] R. H. Swendsen and J.-S. Wang, "Nonuniversal critical dynamics in monte carlo simulations," *Phys. Rev. Lett.*, vol. 58, pp. 86–88, Jan 1987.

[58] A. Iaizzi, "Magnetic field effects in low-dimensional quantum magnets," 2018.

[59] A. B. Owen, *Monte Carlo theory, methods and examples*. 2013.

[60] Z.-X. Li and H. Yao, "Sign-problem-free fermionic quantum monte carlo: Developments and applications," *Annual Review of Condensed Matter Physics*, vol. 10, no. 1, pp. 337–356, 2019.

[61] N. Metropolis and S. Ulam, "The monte carlo method," *Journal of the American Statistical Association*, vol. 44, no. 247, pp. 335–341, 1949. PMID: 18139350.

[62] R. H. Swendsen and J.-S. Wang, "Nonuniversal critical dynamics in monte carlo simulations," *Phys. Rev. Lett.*, vol. 58, pp. 86–88, Jan 1987.

[63] E. Luijten, *Introduction to Cluster Monte Carlo Algorithms*, pp. 13–38. Berlin, Heidelberg: Springer Berlin Heidelberg, 2006.

[64] U. Wolff, "Collective monte carlo updating for spin systems," *Phys. Rev. Lett.*, vol. 62, pp. 361–364, Jan 1989.

[65] "Anders W. Sandvik stochastic series qmc for the s=1/2 heisenberg model." http://physics.bu.edu/~sandvik/trieste12/ssebasic.f90.

[66] O. Derzhko, "Jordan-wigner fermionization for spin-1/2 systems in two dimensions: A brief review," *Journal of Physical Studies*, pp. 49–64, 01 2001.

[67] A. Y. Abul-Magd and M. H. Simbel, "Wigner surmise for high-order level spacing distributions of chaotic systems," *Phys. Rev. E*, vol. 60, pp. 5371–5374, Nov 1999.